AFOSR-TR-97-0667

REPORT DOCUMENTATION PAGE

Form Approved OMB No. 0704-0188

1. AGENCY USE ONLY (*Leave Blank*)	2. REPORT DATE	3. REPORT TYPE AND DATES COVERED
	1 November 1997	Final Technical Report, 15 May 1994 - 31 July 1997

4. TITLE AND SUBTITLE

Fate Assessment of New Air Force Chemicals

5. FUNDING NUMBERS

F49620-94-C-0031

2303/DS

61102F

6. AUTHORS

Theodore Mill and Ronald Spanggord

7. PERFORMING ORGANIZATION NAME(S) AND ADDRESS(ES)

SRI International
333 Ravenswood Avenue
Menlo Park, CA 94025

8. PERFORMING ORGANIZATION REPORT NUMBER

9. SPONSORING / MONITORING AGENCY NAME(S) AND ADDRESS(ES)

Airforce Office of Scientific Research
AFOSR/~~NA~~ NL
110 Duncan Avenue
Bolling AFB, DC 20332-0001

10. SPONSORING / MONITORING AGENCY REPORT NUMBER

11. SUPPLEMENTARY NOTES

12a. DISTRIBUTION / AVAILABILITY STATEMENT

Unlimited Distribution

12b. DISTRIBUTION CODE

13. ABSTRACT (*Maximum 200 words*)

Ammonium dinitramide (ADN) is hydrolytically stable in water at all environmentally relevant pHs from 2-10 at 25°C, with an estimated half life is about 370 years at pH 7. Biotransformation of ADN in water and soil, under aerobic and anaerobic conditions, was not observed. Aqueous and solid ADN photolyzed in sunlight very rapidly, with half lives of a few minutes in summer-fall season, making photolysis the dominant loss process for ADN in surface waters in all seasons.

Quantum yields for ADN photolysis at 285 to 370 nm were 0.1± 0.02 for aqueous ADN solutions and 0.3 to 0.04 between 300 and 325 nm for solid ADN. Major products included nitrite and nitrate ions and nitrous oxide (N_2O), and their proportions were unaffected by oxygen, cation nor wavelength. Solid ADN gave NO, N_2O, N_2 and nitrate ion. Cometabolism with glucose did lead to rapid biodegradation of ADN over 65 hours.

Photolysis and biodegradation of the polyalkylperfluoroether Fomblin Z were evaluated under aerobic and anaerobic conditions. No direct photolysis is possible and no photooxidation with TiO_2 photocatalyst was detected. However, slow release of fluoride ion, found in anaerobic sediments, led to an estimate of 8500 days for the half life of the biodegradation.

14. SUBJECT TERMS

15. NUMBER OF PAGES

16. PRICE CODE

17. SECURITY CLASSIFICATION OF REPORT	18. SECURITY CLASSIFICATION OF THIS PAGE	19. SECURITY CLASSIFICATION OF ABSTRACT	20. LIMITATION OF ABSTRACT
Unclassified	U	U	UL

SRI International

Final Technical Report • October 1997

FATE ASSESSMENT OF NEW AIR FORCE CHEMICALS

SRI Project 6107
Covering the Period 15 May 1994 through 31 July 1997

Prepared by:

Theodore Mill , Minggong Su and Ronald Spanggord
Chemistry and Chemical Engineering Laboratory
and Life Sciences Division

AFOSR Contract No. F49620-94-C-0031
SRI Project 6107

Prepared for:

Air Force Office of Scientific Research
AFOSR/NA
110 Duncan Avenue
Bolling AFB, DC 20332-0001

Attn: Dr. Michael Chipley

333 Ravenswood Avenue • Menlo Park, CA 94025-3493 • (415) 326-6200 • FAX: (415) 326-5512 • Telex: 334486

INTRODUCTION

This final technical report, under Air Force contract F49620-94-C-0031, describes a detailed study of the environmental fate and direct photoreaction of ammonium dinitramide (ADN), an oxidizer for use in next-generation rocket propellants, and a more limited study of the photolytic and biolytic cleavage of polyalkylperfluoroethers, which are thermally stable fluids for advanced aircraft. The third Air Force chemical, quadracyclane, was not studied.

Although extensive data have been developed concerning the optimum synthetic routes preparation, purification and crystallization of ADN as well as sensitivity to deflagration or explosion, essentially no information was available at the outset of this program relevant to the environmental fate of ADN in water or soil.

Dinitramide ion ($-N(NO_2)_2$, DN^-) is a stable inorganic oxidizer, that can be prepared in many different combinations, including the ammonium salt, the dinitramide salt of choice for propellant applications (Schmitt et al., 1993). This study was aimed at reliably predicting the fate of ADN in and on soil and sediment, including rates of hydrolysis, photolysis and biotransformation under different conditions, as well as the reaction products. The detailed photochemical pathways for ADN were also examined.

Photolysis and biodegradation of the polyalkylperfluoroether Fomblin Z were evaluated under aerobic and anaerobic conditions. Photolysis was investigated in water suspension with TiO_2 photocatalyst, while biodegradation used a consortium of microorganisms in natural water-sediment systems. No photoreaction was found based on fluoride ion formation. However, very slow release of fluoride ion was found in anaerobic sediments over 220 days.

BACKGROUND

AMMONIUM DINITRAMIDE

ADN was first discovered (invented) under a secret program in the Soviet Union during the early 1970s, produced in ton quantities and loaded into several types of ICBMs. In the late 1980s, the same class of compounds was rediscovered in the U.S. under a Navy-supported program at SRI (Borman, 1993; Bottaro et al., 1993). The structures of the parent compound, dinitramidic acid and ammonium dinitramide are shown below as I and II

$HN(NO_2)_2$ $NH_4N(NO_2)_2$

I II

Dinitramidic acid is highly acidic with a pK_a of -5. Many of the salts of the acid have been prepared and the ammonium salt (ADN) is now the salt of choice for future propulsion systems.

Determination of the environmental fate for ADN initially was conducted as a screening process to quickly examine how the major loss processes, hydrolysis, photolysis and biotransformation, might compete for ADN (or DN^- ion in dilute, aqueous solution), the simplest situation to interpret. Results from the screening experiments guided the choice of detailed studies to undertake, in this case, photolysis in water and thin films and biotransformation in water and soil.

The U.S. coinventor of ADN, Jeffrey Bottaro of SRI, provided gram amounts of pure ADN and KDN to this study and made them available to other AFOSR investigators in the same program.

POLYALKYLPERFLUOROETHERS

Polyalkylperfluoroethers (PAPFE) are high boiling, inert liquids with very low vapor pressures, useful as hydraulic fluids in next generation aircraft. Fomblin Z and Demnum S65 were supplied by Wright Patterson AFB (L. Gschwender) and have structures III and IV.

$$CF_3(OCF_2)_x(OCF_2CF_2)_yCF_2CF_3$$

III

$$CF_3CF_2CF_2(OCF_2CF_2CF_2)_xCF_2CF_3$$

IV

where X and Y are variable and average molecular weights are 6500 and 4500 for III and IV, respectively. Both PAPFE have densities of 1.84 g/mL. The vapor pressure for III is below 2×10^{-7} torr at 20°C and the decomposition temperature is 350°C (Gschwender, 1995). Fomblin Z (III) should have similar properties.

RESULTS

ENVIRONMENTAL FATE OF ADN

Hydrolysis of Aqueous ADN

Experiments with 150 mM ADN in buffered pH 4,7 and 9 MilliQ water found no change in the concentration of ADN over a period of 37 days in the dark at 60°C. If a maximum of 2% of ADN disappeared in this time (and went undetected), then the half life at 60°C would be >3.5 years. Extrapolation of these data to 25°, assuming that hydrolysis has an activation energy (Ea) of 136 kJ/mole (Hum et al., 1993), gives a half life at 25° of > 45 yrs.

Hum et al. (1993) reported that the hydrolysis of ADN at 150° in unbuffered MilliQ water has a rate constant, k(hydrol) = 4×10^{-4} sec^{-1}. The extrapolated rate constant for hydrolysis at 25°C is 6×10^{-11} sec^{-1}, using their reported E_a of 136 kJ/mole, and the half life is about 370 years, a value not inconsistent with the current estimate of > 43 years. These experiments clearly demonstrate that aqueous DN- ion is indefinitely stable in the dark at 25°C under abiotic conditions.

Photolysis of Aqueous ADN

Photolysis of ADN in sunlight depends on the rate of absorption of sunlight photons above 290 nm (the onset of the solar spectrum) and the quantum yield (efficiency) of the photoreaction. Equation (1) defines the rate constant for photolysis in terms of the uv/vis spectrum, the solar intensity and the quantum yield, Φ.

$$k_p = 2.303\Phi\Sigma\varepsilon_\lambda Z_\lambda / j \qquad (1)$$

where ε_λ and Z_λ are the extinction coefficient for ADN at wavelength λ and solar intensity, at wavelength λ respectively and j is a unit for converting photons to einsteins (Zepp and Cline, 1977). Determination of these values is discussed below.

UV Spectrum of ADN. Aqueous ADN absorbs near-uv light strongly from 295 nm (the onset of the solar spectrum) to beyond 370 nm. As expected, ADN and KDN (the potassium salt) have identical uv spectra. The spectrum of ADN is plotted in Figure 1 along with the sunlight

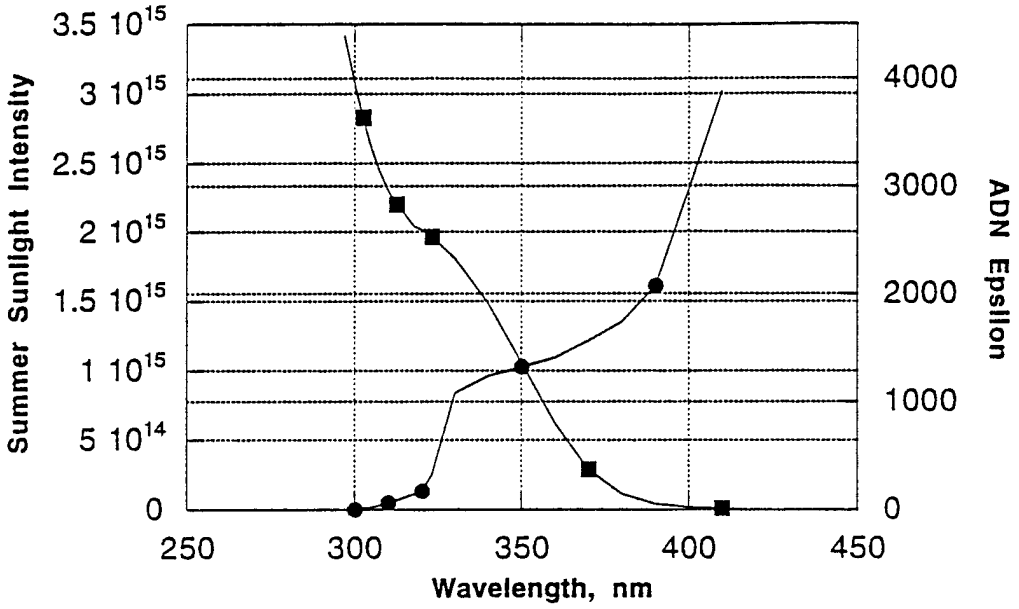

Figure 1. UV spectrum of ADN in water with the sunlight emission spectrum.

emission spectrum. The overlapping region of the two curves is defined in Equation (1) as $\Sigma\varepsilon_\lambda Z_\lambda$ and values of $\varepsilon_\lambda Z_\lambda$ over the entire spectral region are listed in Table 1. Figure 2 shows the sunlight action spectrum of ADN as a plot of $\varepsilon_\lambda Z_\lambda$ versus wavelength. The action spectrum has a maximum near 330 nm, assuming that the quantum yield is the same over the entire absorption spectrum (see below), indicating that the fastest rate of photolysis occurs with photons near 330 nm because the rate of photon absorption, as well as sunlight intensity are high and the product of the two parameters ($\Sigma\varepsilon_\lambda Z_\lambda$) is maximized at 330 nm (see Table 1).

Table 1

CALCULATION OF $\Sigma Z_\lambda \varepsilon_\lambda$ FOR ADN AT 40° LAT. MIDSUMMER [a]

Wavelength Center, nm	Z_λ (Summer) Photons cm^{-2} s^{-1} [b]	ε_λ $M^{-1}cm^{-1}$	$Z_\lambda \varepsilon_\lambda / j$ s^{-1}	$\Sigma Z_\lambda \varepsilon_\lambda / j$ [c] s^{-1}
297.5	7.16e+11	4424	5.28e-6	5.28e-6
300.0	2.40e+12	4194	1.68e-5	2.21e-5
302.5	7.23e+12	3871	4.66e-5	6.87e-5
305.0	1.81e+13	3364	1.01e-4	1.70e-4
307.5	3.05e+13	3180	1.62ee-4	3.32e-4
310.0	4.95e+13	2949	2.43e-4	5.75e-4
312.5	7.17e+13	2857	3.41e-4	9.17e-4
315.0	9.33e+13	2719	4.23e-4	1.34e-3
317.5	1.15e+14	2673	5.12e-4	1.85e-3
320.0	1.35e+14	2350	5.29e-4	2.38e-3
323.1	2.52e+14	2595	1.06e-3	3.44e-3
330.0	8.46e+14	2350	3.31e-3	6.76e-3
340.0	9.63e+14	1982	3.18e-3	9.94e-3
350.0	1.03e+15	1429	2.45e-3	1.24e-2
360.0	1.10e+15	876	1.61e-3	1.48e-2
370.0	1.22e+15	419	8.53e-4	1.52e-2
380.0	1.35e+15	166	3.73e-4	1.54e-2
390.0	1.61e+15	55	1.48e-4	1.54e-2
400.0	2.31e+15	18	6.74e-5	1.55e-2
410.0	3.02e+15	5	2.32e-5	1.55e-2
420.0	3.10e+15	7	3.62e-5	1.55e-2
430.0	2.98e+15	5	2.48e-5	1.55e-2
440.0	3.51e+15	0	0	1.55e-2

[a]Column 2 data are from Zepp and Cline (1977).

[b]These values are the running sums of Column 4 values; the last value is total $\Sigma Z_\lambda \varepsilon_\lambda$.

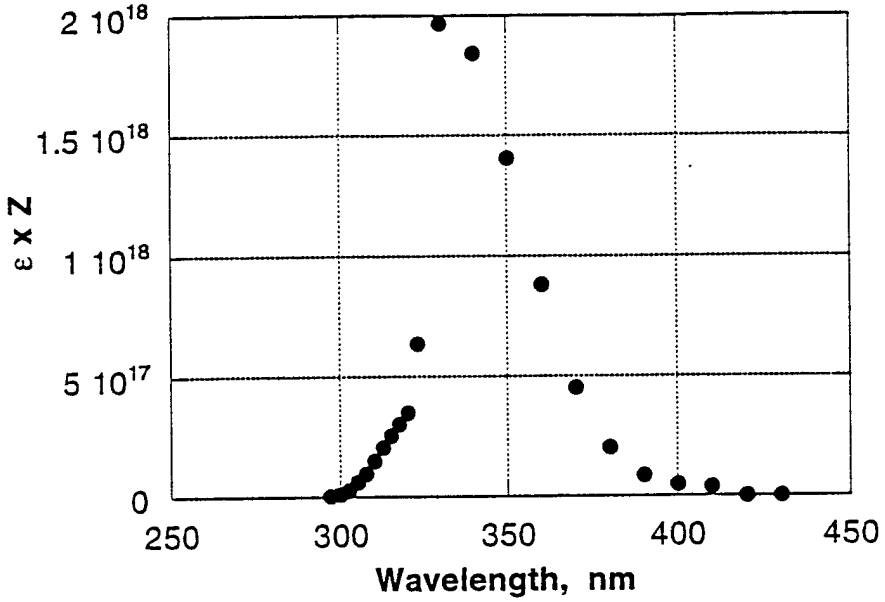

Figure 2. Action spectrum for aqueous ADN: λ_{max} = 330 nm.

The uv spectrum of ADN can be used to estimate the theoretical maximum rate of photolysis in dilute aqueous solution by assuming that Φ is one. The value is for solar noon.

$$k_p(max) = 2.303\Sigma\varepsilon_\lambda Z_\lambda/j \qquad (2)$$

From Table 1, $\Sigma\varepsilon_\lambda Z_\lambda/j$ for ADN is 0.015 s^{-1}, corresponding to a value of $k_p(max)$ = 0.0345 s^{-1}. Thus, the theoretical minimum half life for ADN in sunlight is ($0.693/k_p(max)$) about 20 seconds in summer noon sunlight at 40° N latitude.

Photolysis Kinetics of ADN. Experiments with 10-40 μM aqueous ADN demonstrated that it rapidly photolyzed in sunlight by a first order loss process, making photolysis the dominant environmental loss process for ADN or any other DN- ion salt. Figure 3 shows the loss of ADN in June sunlight. The data were well fitted to a simple first order exponential curve giving k_p = 0.218 min^{-1} and $t_{1/2}$ = 3.2 min for 10-40 μM ADN in summer sunlight close to three minutes. The sunlight-averaged quantum yield (Φ) is 0.1 based on Equation (1) and the value of $\Sigma\varepsilon_\lambda Z_\lambda$ from Table 1. This average value of Φ is convenient for estimating the half life of ADN under a variety of other conditions, including changes in time of day and year and under cloud cover. Z_λ values at 40°N lat. in winter, spring, summer and fall, half life of ADN can be estimated for the whole year as shown in Figure 4.

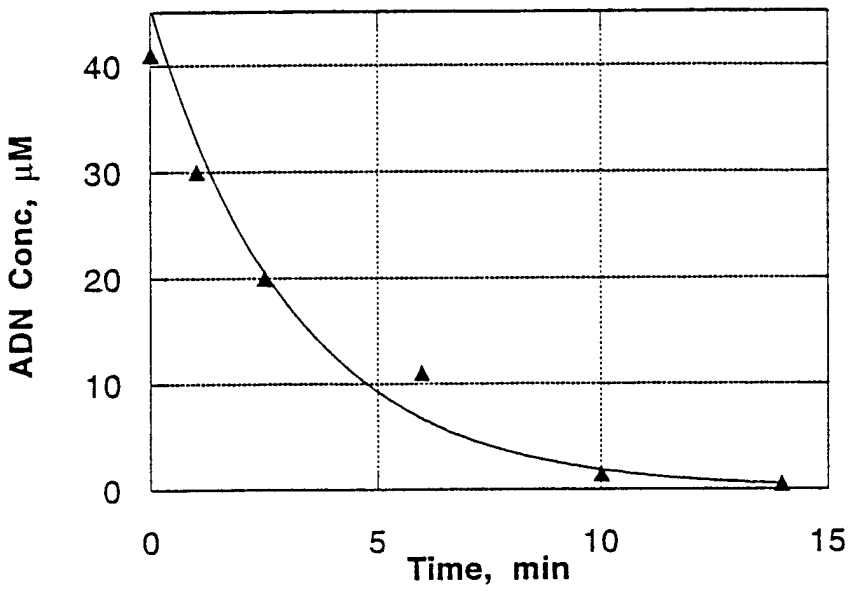

Figure 3. Photolysis of 40 µM ADN in June sunlight 38°N Lat Data fitted to exponential form y = nexp(-0.218t)

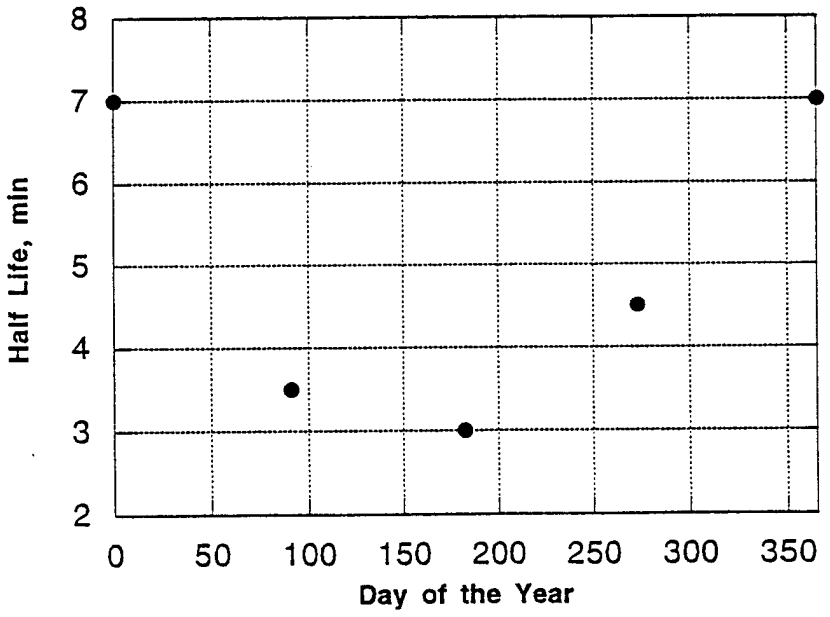

Figure 4. Calculated half life of ADN at 40° Lat over four seasons.

Quantum Yield Measurements. The quantum yield for photolysis of aqueous ADN as a function of wavelength was measured in five narrow wavelength intervals using a monochrometer to isolate wavelengths from a 450 W xenon lamp and filters to minimize stray light. Values for Φ ranged from 0.16 at 284 nm to 0.12 at 370 nm. This is a considerably narrower range of values than those reported by Beretvas et al. (1995), but they are in good agreement with the measured sunlight-averaged value of 0.1 (above). Table 2 summarizes quantum yield data.

Table 2

QUANTUM YIELDS FOR PHOTOLYSIS OF ADN

Wavelength, nm (±5 nm)	$10^{-14}I_o$, Photons s^{-1}[a]	10^4k_p, s^{-1}[b]	Quantum Yield[c]
284	2.13	6.80	0.16
300	2.92	5.72	0.13
325	5.37	5.46	0.11
350[d]	8.42	5.11	0.11
370[e]	11.5	2.15	0.12
Sunlight	9.8×10^{4}[f]	340	0.1

[a]Incident intensity on photolysis tube at stated wavelength from a 450 w xenon lamp and 1/4 m monochrometer (1200 l/mm).
[b]From first-order plot of loss of 20 mM aqueous ADN.
[c]Defined as moles of ADN photolyzed/einstein of photons absorbed.
[d]Monochromator light filtered through 1 cm pure acetone.
[e]Monochromator light filtered through 1 cm pure acetone containing 2% acetophenone.
[f]Total solar flux in photons cm^2 s^{-1}.

Photolysis Products. Aqueous photolysis of ADN produced three products: NO_3^-, NO_2^- and N_2O; ammonium ion was not consumed and NO and N_2 were not found. These products accounted for ~100% of the nitrogen in photolyzed ADN. Table 3 summarizes several experiments conducted with sunlight, or a xenon lamp or 308 or 370 nm lasers, as well helium and argon in place of air. While neither argon, nor pH changed the rate of photolysis, nor did photolysis wavelength affect products, changes in pH did dramatically affect the product ratio. Table 4 shows a summary of product formation at pH 2-11, normalized to conversion of one µmole of ADN. Figure 5 plots product yields for 40 µM ADN solutions photolyzed for 4 min to 65 to 70% conversions at seven pH between 2 and 12 in air and Table A.1 provides detailed

product analyses for these experiments. Nitrogen mass balances in almost all of the experiments were greater than 85%.

Table 3

PHOTOLYSIS EXPERIMENTS WITH AQUEOUS KDN/ADN[a]

[DN], μM[b]	Conditions	N_2O %	% Conversion	NO_2^- %	NO_3^- %	NO_2^-/NO_3^- Ratio	N Balance[c] %
K915	sun/Ar	42	100	18.9	22.5	0.8	88
K300	sun/Ar	25	100	33.3	22.7	1.5	81
A1050	sun/Ar	21[d]	100	20.2	21.2	1.0	63
A1050	sun/air	11[d]	86	26.8	20.9	1.3	59
K1080	sun/air	14[d]	80	26.6	20.4	1.3	61
A1050	sun/air	19[d]	79	27.1	20.1	1.4	66
A1050	sun/Ar	16[d]	86	25.7	19.9	1.3	62
A1060	sun/He	46	100	30	25	1.2	100
A1060	sun/He	37	71	37	28	1.3	102
A1060	sun/He	45	51	39	27	1.5	111
K500	308nm/air	32	48	21.5	31.3	0.7	85
K980	308nm/air	NA	63	19.2	77.8	0.3	-
K980	308nm/air	NA	76	13.8	36.3	0.4	-
K980	370nm/air	30	51	22.4	24.4	0.9	76
K980	370nm/air	30[e]	51	28.1	22.4	1.3	80

[a]All analyses are duplicates withstand dev. of 0.1% for KDN/ADN, 0.2% for nitrite and nitrate and 1% for N_2O.
[b] Cation, μM concentration
[c]Calculated on consumed DN^- (no NH_4^+ consumed): balance = $(NO_2^- + NO_3^- + 2N_2O)/\Delta DN^-$.
[d] N_2O values underestimate yields in these experiments.
[e]Assumes same yield of N_2O as in duplicate.

Table 4

PRODUCTS FROM AQUEOUS ADN PHOTOLYSIS AT pH 2-11[a,b]

pH	Δ DN^- ⟶	N_2O	NO_2^-	NO_3^-	ΣNO_x^-	ΣN[c]
2	1	0.94	0.3	1.0	1.30	3.2
5	1	0.68	1.3	0.58	1.88	3.2
9	1	0.54	1.8	0.27	2.07	3.2
11	1	0.41	2.2	0.13	2.33	3.2

[a]All concentration are in mmoles, normalized to conversion of 1 mmole of ADN. [b]No effect of vigorous purging with argon. [c]No change in NH_4^+.

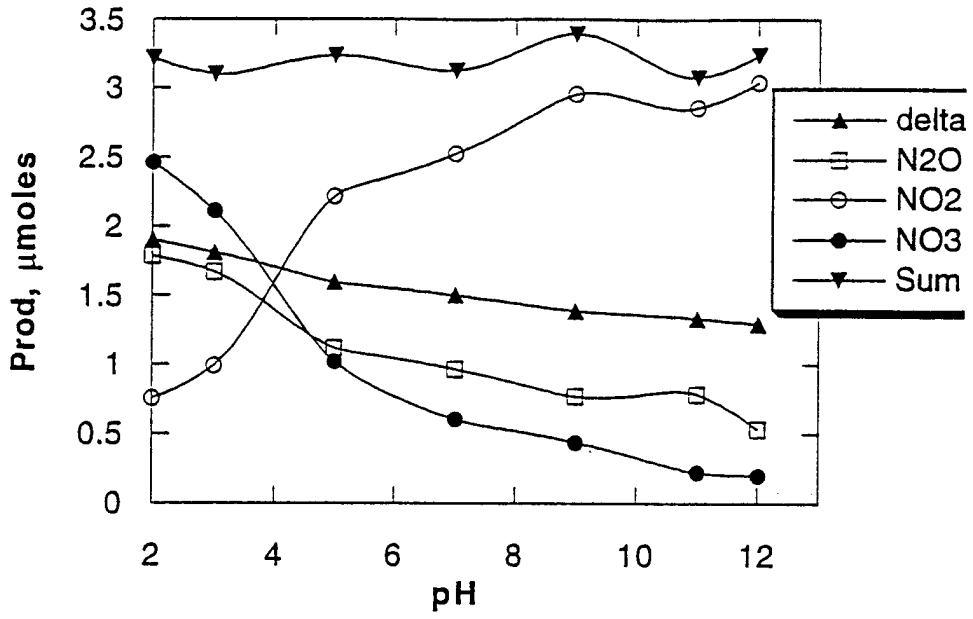

Figure 5. Changes in product composition with change in pH for photolyzed aqueous ADN.

The most important effect of pH was to change the relative amounts of NO_2^- and NO_3^- formed; at pH 11, the ratio of NO_2^-/NO_3^- was over 20, but at pH 2, the ratio declined to 0.5. To exclude the possibility that NO or NO_2 was formed and produced NO_2^- and NO_3^-, vigorous argon purging was used to remove any NO formed as during photolysis. Purging had no effect on rates, products or pH effects. Moreover, experiments with NO_2 added to water at pH 3, 7 and 11 showed no effect of pH on the close ratio of NO_3^- to NO_2^- arising from hydrolysis of NO_2. These results all but eliminated NO or NO_2 as proximate intermediates in formation of NO_3^- and NO_2^- from ADN.

Similar sets of pH experiments were also conducted with KDN, with a similar effect of pH on the ratio of NO_3^- to NO_2^-. However, at the same pH, the ratio of NO_3^- to NO_2^- also changed when argon replaced air in the reaction mixture. Detailed product data for KDN pH experiments are listed in Table A.2.

Photolysis in Organic Solvents. Photolysis rates and products for 100 µM ADN solutions in four other, dry solvents in which ADN was readily soluble were also examined. Photolysis of these solutions in borosilicate tubes exposed to a xenon lamp, gave rates in all solvents within ±25% of the rate in water and formed nearly equal amounts of NO_2^- and NO_3^-. Table 5 summarizes the results. Photolysis in acetone was particularly informative, because

acetone effectively adsorbs all UV radiation below 335 nm, thereby eliminating >80% of the light absorbed by ADN. The fast rate observed in acetone implicates a triplet sensitized photoprocess in which acetone absorbs most of the light, but efficiently transfers the energy to ADN via triplet-singlet interaction in an indirect photoprocess. None of the other solvents in Table 5 absorbs much near uv light, therefore these other reactions appear to be direct photoreactions.

Table 5

SOLVENT EFFECTS ON ADN PHOTOLYSIS[a]

Solvent	Conversion, %	Rate, μM/min	NO_2^-/NO_3^-
Water (pH 7)	53	8.3	4
Methanol	49	8.2	1.3
Acetone	60	10	1.1
DMF	76	13	-
Acetonitrile	62	13	1.1[b]

[a]Photolyzed in air with a xenon uv source with 100-110 μM ADN.
[b]KDN had a ratio of 0.8 for the same conversion.

A more detailed examination of the time course of photolysis of 25 mM ADN in acetonitrile gave results plotted in Figure 6. Nitrate ion appears to grow while nitrite decreases and N_2O remains a small component throughout the reaction. These results are consistent with results described below for solid ADN photolysis wherein nitrite must rapidly form and then disappear by reaction with NH_4^+. Changes in NH_4^+ or N_2 formation in acetonitrile experiments were not determined.

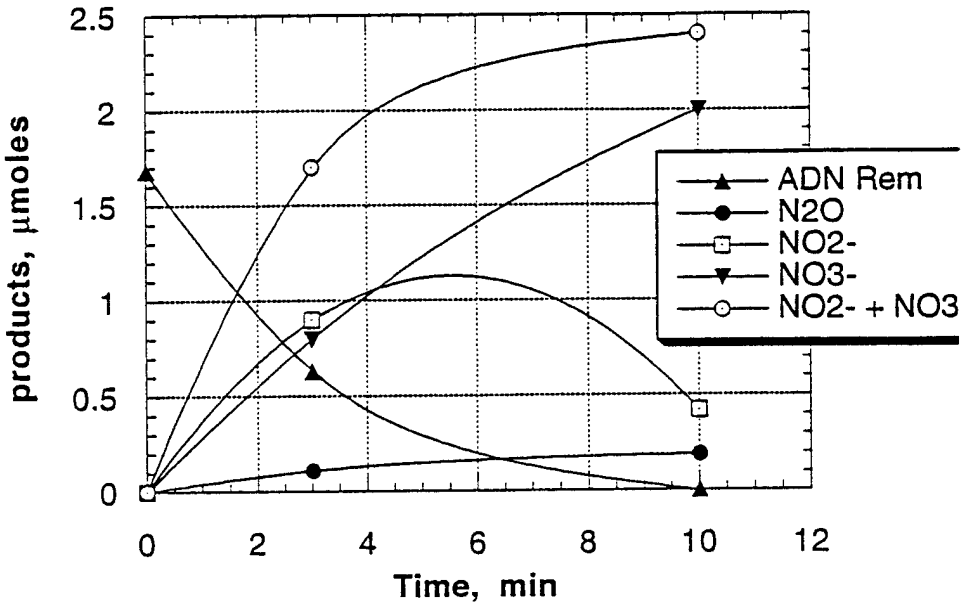

Figure 6. Photolysis of 50 µM ADN in acetonitrile as a function of time.

Photolysis of Solid ADN

A wide range of experiments were conducted with ADN and KDN as thin films cast on quartz tubes and photolyzed with a xenon source in air, argon or carbon dioxide (to detect and measure nitrogen formation). Films were cast from acetone or methanol and photolyzed for periods corresponding to 20-100% conversions. Tables 6 shows that a different mixture of products formed from solid ADN, compared with aqueous solutions of ADN and details the products found, along with control films retained in the dark.. Major products from photolysis were NO_3^-, NO, N_2O and N_2, with only very small amounts of NO_2^-. Formation of N_2 was accompanied by concomitant loss of NH_4^+, suggesting that N_2 formed as the result of a redox reaction between NH_4^+ and NO_2^-. This was confirmed by finding that KDN did form NO_2^-, but gave no N_2, as shown in Table 7.

Figures 7-9 show the formation of products in ADN and KDN thin film photolysed over a range of conversions. Figure 7 shows the growth of nitrogen at the expense of ammonium ion with no growth of nitrite. Figure 8 plots NO_3^-, NO_2^-, N_2O and NO in the same experiment. Nitrite barely changes, whereas NO_3^- and N_2O increase with conversion. Figure 9 shows that KDN photolyzes to form nearly equal amounts of NO_3^-, NO_2^- and NO; N_2O appears to lag, but that may be an analytical artifact .

Table 6

PHOTOLYSIS OF ADN THIN FILMS IN CO_2[a]
(All concentration units in μmoles)

ADN init.	ADN Final	Δ ADN	N_2O	N_2	NO	NO_2^-	NO_3^-	NH_4^+ consum	ΣN	N mass Bal %
19.35	13.69	5.66	1.85	6.97	2.66	2.24	2.46	3.57	17.42	84.8
19.35	6.40	12.95	5.92	11.56	4.64	1.86	8.04	6.18	41.89	93.0
19.35	3.53	15.82	7.54	11.79	8.12	2.17	11.69	6.49	53.04	98.3
19.35[b]	19.32	0.04	0.00	3.80	0.00	0.00	0.00	0.00	0.00	0.0
19.35[b]	19.24	0.11	0.00	3.28	0.00	0.00	0.00	0.00	0.00	0.0

[a]Photolyzed 0.1-0.2 μM films under CO_2 using a 450 W xenon lamp in 34 mL quartz tubes for 40 or 60 min. [b]Dark control.

Table 7

PHOTOLYSIS OF KDN THIN FILMS IN CO_2[a]
(All concentration units in μmoles)

KDN init.	KDN Final	Δ KDN	N_2O	N_2•	NO	NO_2^-	NO_3^-	ΣN	N mass Bal %
14.07	4.73	9.34	3.29	4.16	4.35	6.56	5.67	23.15	82.7
14.07	4.52	9.55	3.74	4.07	7.73	7.28	5.26	27.75	96.9
14.07	3.72	10.35	3.34	9.98	6.63	7.58	6.90	27.78	89.5
14.07[b]	14.07	0.00	0.00	9.40	0.00	0.00	0.00	0.00	0.0
14.07[b]	14.19	-0.12	0.00	3.42	0.00	0.00	0.00	0.00	0.0

[a]Photolyzed 0.1-0.2 μM films under CO_2 using a 450 W xenon lamp in 34 mL quartz tubes for 40 or 60 min. [b]Dark control.

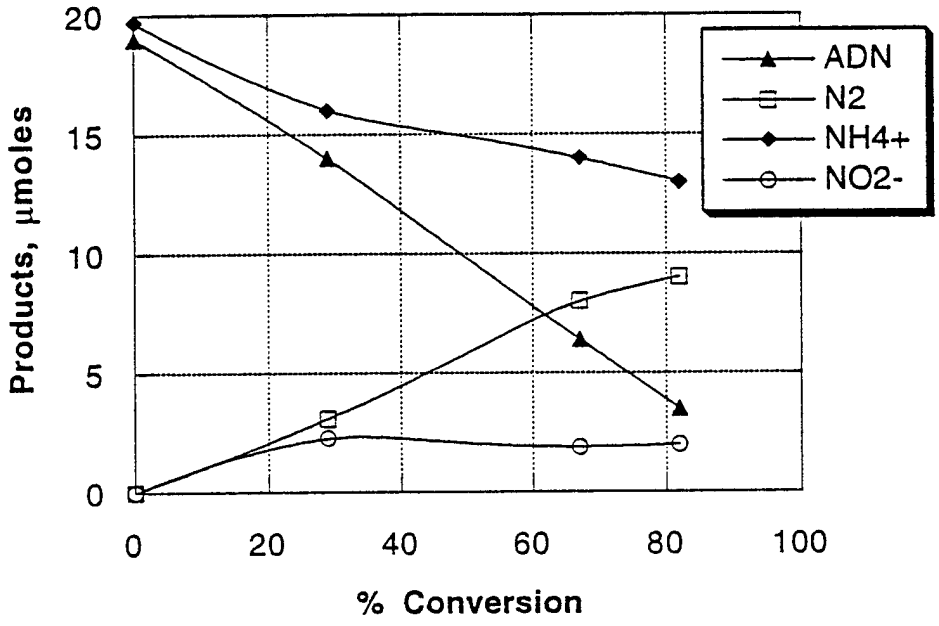

Figure 7. Photolysis of 0.1 mM ADN film: loss of ADN and NH_4^+ and formation of N_2 and NO_2^-.

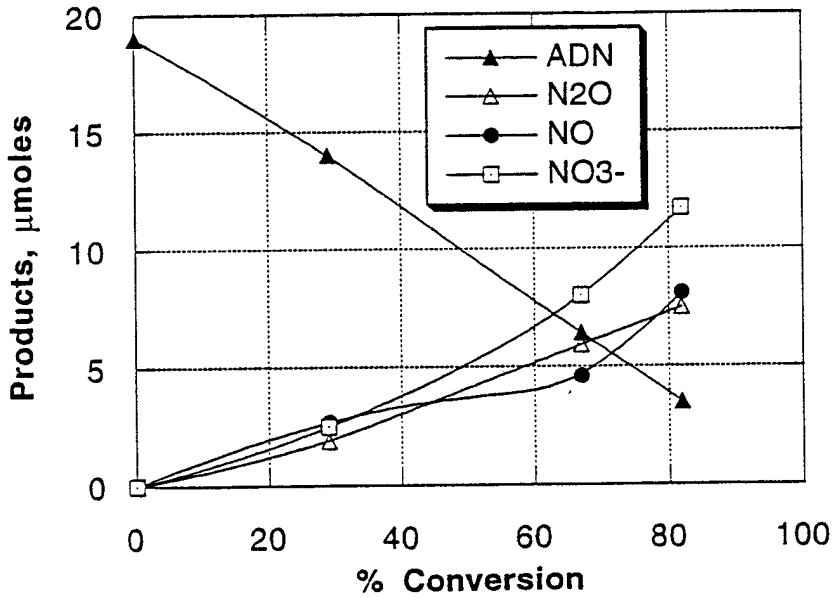

Figure 8. Photolysis of 0.1 µM ADN film: loss of ADN and formation of N_2O, NO and NO_3^-.

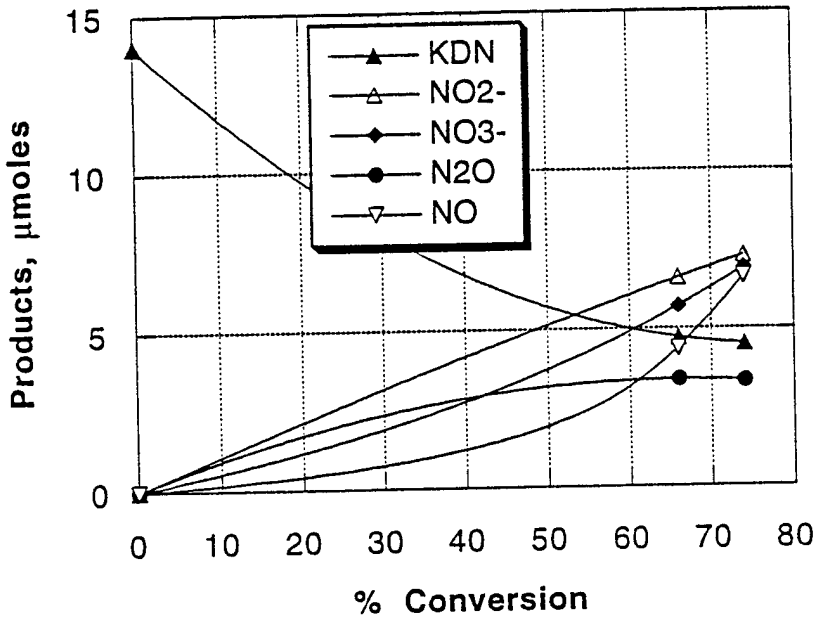

Figure 9. Photolysis of 0.1 µM KDN film: loss of KDN and formation of products.

^{15}N-Labeled ADN Experiments. To learn more details of the ADN solid state photolysis pathways, a collaborative study was conducted with Lawrence Merwin of the China Lake Naval Weapons Center using $NH_4{}^{15}N(NO_2)_2$ supplied by Merwin to determine the origins of NO_3^-, NO and N_2O produced on photolysis. Four experiments were conducted in a 1100 mL cylindrical borosilicate reactor surmounted with a 1 cm tube with a 5 mm dia bore. Uniform 0.73 µm thin films of from 70 mg of ADN were coated on the vertical walls of the reactor and the reactor was purged of air with argon or CO_2. In two experiments, $NH_4{}^{15}N(NO_2)_2$ or $NH_4{}^{14}N(NO_2)_2$ was photolyzed to 70-90% conversion in flowing argon to sweep NO out and eliminate subsequent formation of NO_3^- from NO via hydrolysis of NO_2. The residual film was dissolved in D_2O and analyzed for NO_3^-, NO_2^- and ADN by ion chromatography. No NO_2^- was detected. The ^{15}N nmr spectrum, shown in Figure 10, has a peak at -0.2 ppm attributed to $^{15}NO_3^-$ corresponding to less than 12% of the total NO_3^- formed in the reaction mixture. The ^{15}N nmr spectrum of starting $NH_4{}^{15}N(NO_2)_2$ has a triplet with the center peak at -56.12 ppm and contained less than 2% $NH_4N(^{15}NO_2)_2$, whereas $^{15}NH_4^+$ has a peak at 355.6 ppm. In effect, over 80% of the ^{15}N label was missing from water soluble products.

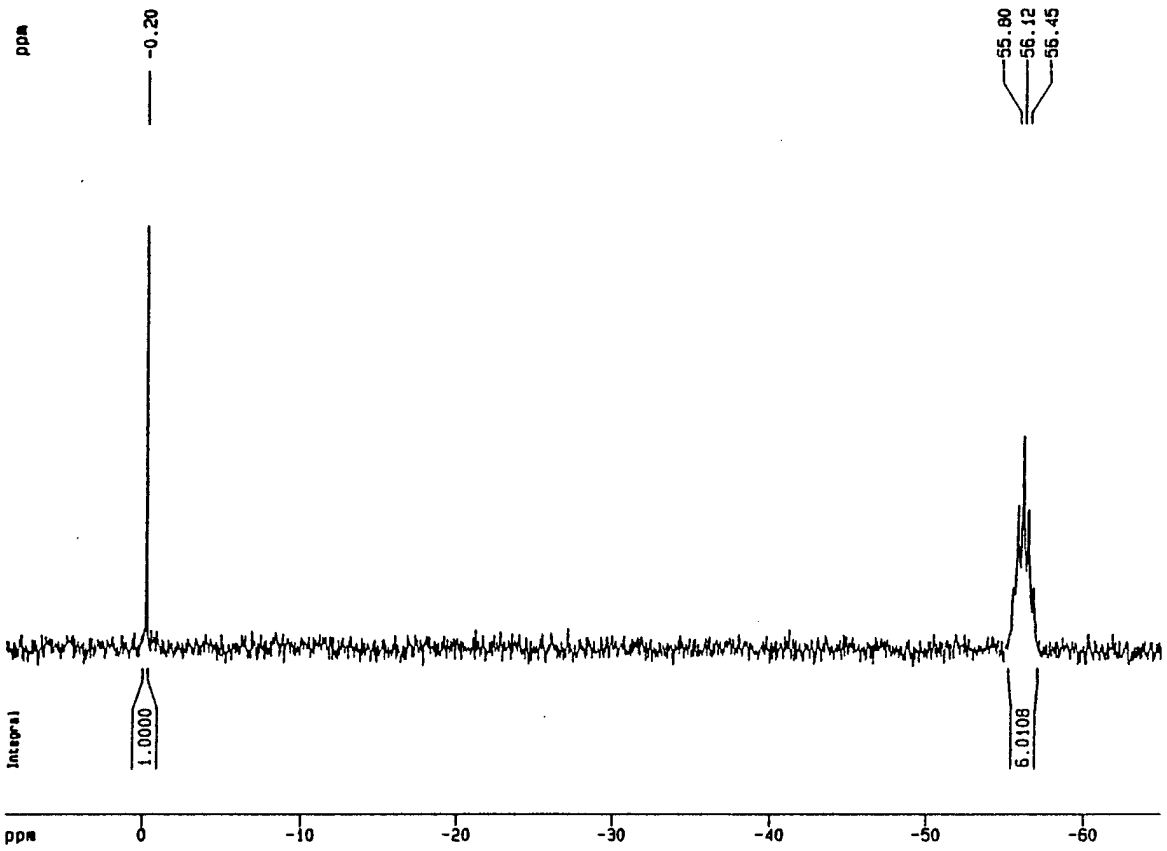

Figure 10. ^{15}N NMR spectrum of NO_3^- from ^{15}N ADN photolysis.

Two other experiments with $^{15}N^-$ and $^{14}N^-$ labeled ADN under static argon and CO_2 were analysed for N_2O, NO and N_2 by gas chromatography. Results of these experiments are listed in Table A.3. The isotopic composition of NO and N_2O in these experiments was determined by FTIR (N_2 is IR silent). Thin films of ADN and KDN were coated onto a 3 cm diameter quartz cylinder, then inserted into a 5 cm dia infrared gas cell fitted with gas inlet and outlet valves and detachable NaCl windows. After purging the cell with argon, the ADN or KDN thin film was photolyzed for 20-50 min with a xenon lamp to convert 70-80% of the DN^- salt.

The FTIR spectrum of the gaseous photolysis products showed that NO_2, detectable at very low concentrations in the IR, was not a primary product from photolysis of solid ADN in an argon or carbon dioxide atmosphere. The only IR peak initially observed was that of N_2O and the peak positions of N_2O in ^{15}N-ADN and ^{14}N-ADN photolyses were different. Whereas $^{14,14}N_2O$ has peaks at 2237 and 2213 cm^{-1}, $^{15}N^{14}NO$ has peaks at 2213 and 2190 cm^{-1} (determined with authentic ^{15}NNO prepared by pyrolyzing $^{15}NH_4NO_3$ in the gas cell). The N_2O spectrum found from ^{15}N ADN corresponded well with authentic ^{15}NNO, as shown in Figure 11; $N^{15}NO$ has a

different doublet position. However the ^{15}N balance from ^{15}NNO accounted for only half the original ^{15}N in ADN, based on the data from Table A.3, where 400 μmoles of ADN gave 212 μmoles N_2O, 231 μmoles NO and 167 μmoles of N_2. NO could account for the almost 200 μmoles of missing ^{15}N, however Figure 11 shows that NO is ^{14}NO not ^{15}NO.

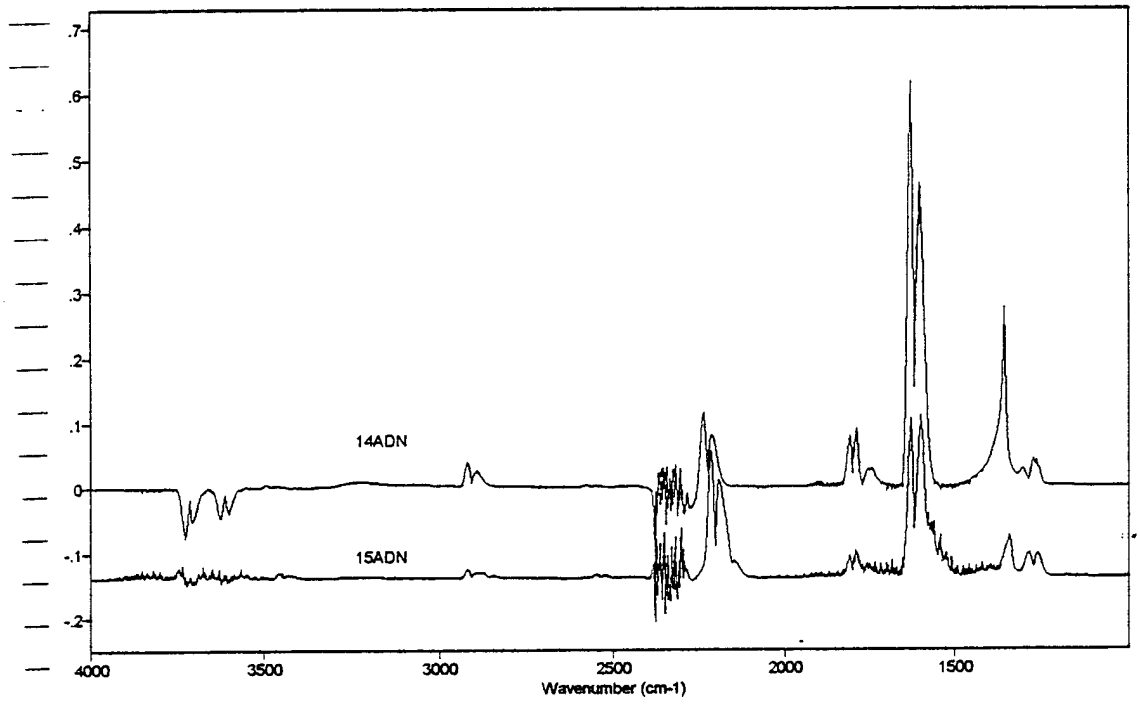

Figure 11. FTIR gas phase spectrum of N_2O and NO derived from photolysis of ^{14}N-ADN and ^{15}N-ADN thin films. Peaks: 14,14 N_2O: 2237/2213 cm^{-1}; 15,14 NNO: 2213/2190 cm^{-1}; 14,15 N_2O: 2190/2165 cm^{-1}; 14 NO_2: 1628/1601; 15 NO_2: 1594/1566.

The NO IR band is too weak to observe directly. However, after injecting excess oxygen into the reaction cell, prompt formation of a strong doublet NO_2 band at 1628 and 1601 cm^{-1} was diagnostic for NO formation and formed the basis for characterizing the isotopic composition of NO. The NO_2 IR peaks formed from ^{14}N- and ^{15}N-ADN were identical (Figure 11), showing that NO had no ^{15}N label. IR bands for HONO (1808 and 1790 cm^{-1}) and NO_3^- (1780 cm^{-1}, deposited on the salt windows) also formed as a result of hydrolysis of NO_2 on the surfaces by water produced in the redox reaction of NH_4^+ with NO_2^-. Water was removed from most FTIR photolysis experiments by adding $CaSO_4$ particles to the IR cell, minimizing formation of HONO and NO_3^- ion.

To confirm the isotopic identity of NO_2 formed from ^{15}N-ADN, authentic $^{15}NO_2$ was prepared from Li $^{15}NO_3$ by pyrolysis and transferred to the FTIR cell. Figure A1 shows the comparison of IR spectra for $^{14}NO_2$ and $^{15}NO_2$ with the spectrum for NO_2 formed from ^{15}N-ADN. Spectra of NO_2 from ^{15}N-ADN and ^{14}N-ADN coincide exactly at 1627 and 1605 cm^{-1}, whereas the spectrum of $^{15}NO_2$ is shifted to 1594 and 1566 cm^{-1}. However, spectrum of NO_2 from ^{15}N-ADN has a different intensity ratio for the 1627 and 1605 cm^{-1} peaks from that of authentic $^{14}NO_2$ (from ADN), raising the possibility that the ^{15}N-ADN derived NO_2 has 10-15% $^{15}NO_2$ in the $^{14}NO_2$.

The results from the coupled FTIR and GC analyses suggest that the missing half of ^{15}N was initially formed as $^{15}NO_2^-$, a transient in the solid phase, going on to form N_2 (as $^{15}N^{14}N$) from NH_4NO_2 and that $^{15}NO_2^-$, which must have formed in nearly equimolar amount to photolyzed ADN, would account for the missing ^{15}N.

Actinometry of ADN Thin Films. Quantum yields for photolysis of solid ADN thin films were determined at 300 and 330 nm by measuring the total photon flux in ferrioxalate solutions, with and without ADN thin films interposed in the light beam. From the difference in photon flux as ADN photolyzes, the absorbed photon flux in the film could be estimated and, with measured loss of ADN, used to calcualte the apprarent quantum yields. The measured quantum yields at 300 and 330 nm were 0.36 and 0.04 respectively, larger and smaller than the values for aqueous ADN. The films were cast with special care to ensure maximum transmissivity and minimum reflectivity. Nonetheless, some light was undoubtedly scattered at the surface and lost to the ferrioxalate solution, with the effect of decreasing the apparent quantum yield. Since scattering usually increases with decreasing wavelength, the results are not readily interpreted as being due to surface relectivity.

Low Temperature Photolysis. The purpose of photolysing solid ADN at low temperatures was to determine if one or more unstable (at 25°C) intermediates form that react by thermal pathways to give observed final products. At -100°C these intermediates, such as initial free radical partners that might live long enough top retard production of NO and N_2O. Photolysis reactions were conducted using ADN coated on internal walls of a borosilicate vessel, sealed under argon and placed inside a transparent quartz Dewar cooled with pentane-liquid nitrogen slush to -100° to -130°C. The same system was used to photolyze a control ADN film at 25°C.

Photolysis reactions converted nearly 70% of ADN at -100° and 25°C. Gas products, sampled at -100°C, were analyzed by GC and then reanalyzed after the mixture was warmed to

25°C and then recooled to -100°C to compare the results with ADN photoproducts formed at 25°C. The composition of -100°C mixture was unchanged by warming to 25°C and recooling. Moreover, 25° and -100°C product compositions (measured at 25°C) were very similar: 7.6 μmoles of ADN photolyzed at -100°C gave (at -100°C) 3 and 7.3 μmoles of N_2O and NO respectively, whereas 6.2 μmoles of ADN photolyzed at 25°C gave 1.8 and 7.2 μmoles of N_2O and NO respectively.

The same samples also formed 0.13 and 5.5 μmoles of NO_2^- and NO_3^- respectively at -100°C, compared with 0.11 and 2.7 μmoles respectively at 25°C. The difference between NO_3^- yield could be important, but overall the results suggest that any excited state species promptly formed final products and any nitrite ester was a small proportion of the total transformed product mixture. Additional low temperature experiments are needed to more clearly characterize the presence of intermediates.

BIOTRANSFORMATION OF ADN

The biotransformation of ADN was investigated in a fresh eutropic pond water/sediment mixtures under both aerobic and anaerobic conditions. Five g of Searsville Pond sediment (Stanford, CA) and 110 mL of Searsville Pond water with ~10 ppm (80 μM) ADN was purged with synthetic air or nitrogen to establish aerobic or anaerobic conditions in 250 mL Micro-Oxymax chambers. The aqueous phase were stirred and samples were removed periodically, centrifuged, and analyzed for ADN by liquid chromatography. No loss of ADN in the aerobic system (14.1 ppm) or the anaerobic system (8.8 ppm) was observed after 60 days of incubation. These results indicate that either ADN is toxic to the organisms or that they have no need to utilize ADN as a nitrogen source.

ADN loss was also investigated in the presence of Tripticase soy medium (TSM) with variable ADN concentrations. In the presence of 500 ppm TSM and high ADN concentrations, ADN was lost over a sixteen day period (Figure 12) and followed pseudo first-order kinetics (Figure 13). At 100 ppm (0.8 mM), ADN was lost much more slowly and no loss was observed with 10 ppm ADN with 5.0 μL of TSM. Thus, it appears that ADN is not toxic to aquatic organisms, however, they need additional nutrients to metabolize ADN.

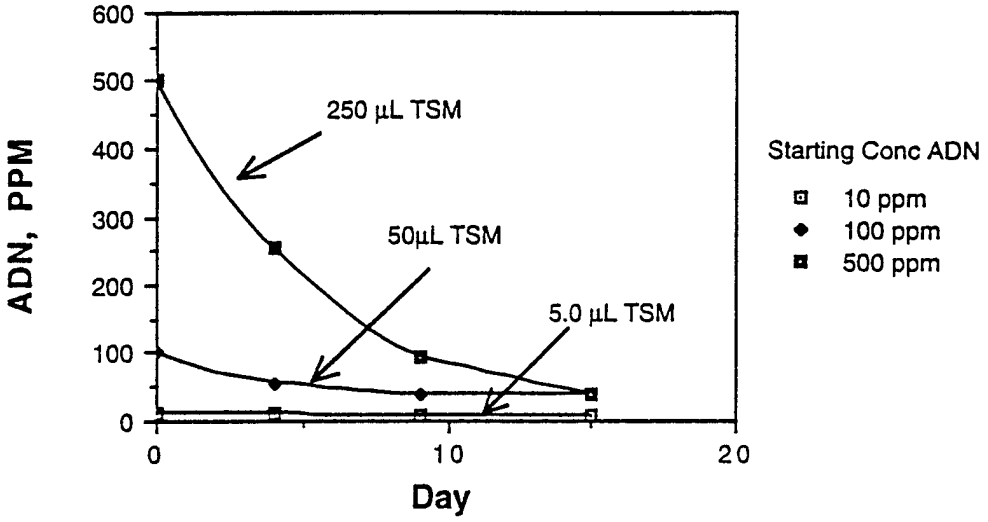

Figure 12. ADN loss with added TSM.

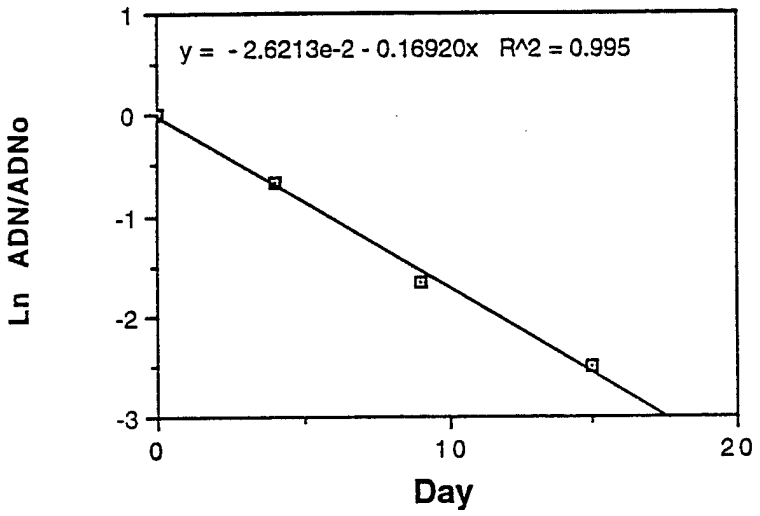

Figure 13. Pseudo first-order loss plot for ADN with 250 µL TSM.

Glucose (1%) also enhanced the loss of ADN: 20 ppm (160 µM) of ADN disappeared in 65 hours while suspensions without glucose showed no ADN loss (Figure 14). When the glucose concentration was varied, there was little difference in the rate of ADN loss at 0.5% versus 1% (Figure 15).

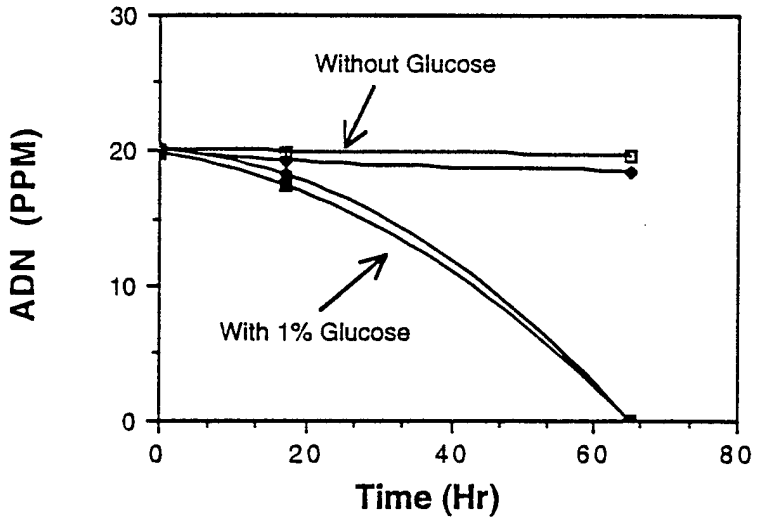

Figure 14. ADN loss in the presence and absence of 1% glucose.

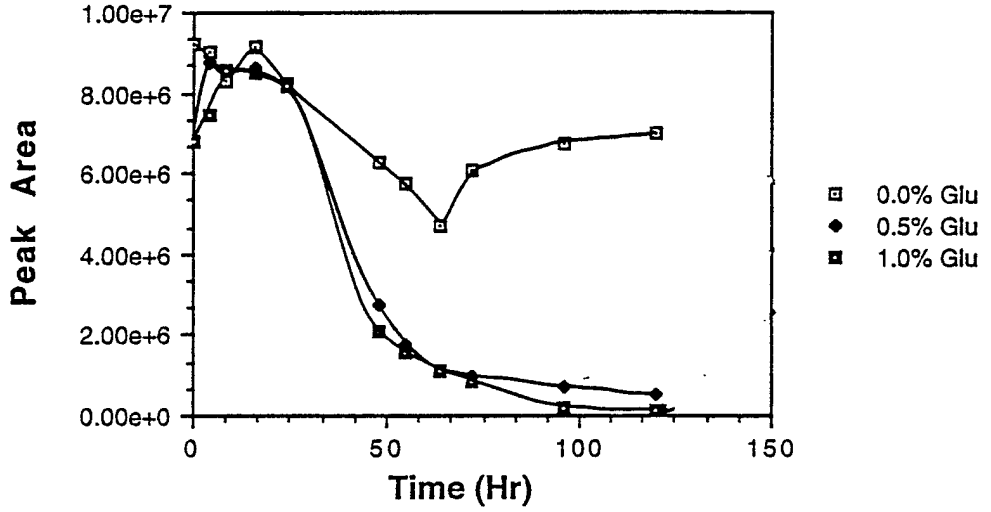

Figure 15. ADN loss as a function of glucose concentration.

No transformation products, including nitrate and nitrite, were observed in the HPLC profiles or by ion chromatography in studies with added nutrients. To test for production of ammonia, Searsville pond sediment and 20 ppm KDN were mixed with a basal salts medium (ammonium free) and glucose. KDN was degraded with a half life of 81 hours in a first order process, as shown in Figure 16. Ammonia formed from KDN but at very low concentrations and disappeared again (Figure 17), suggesting that the ammonia was utilized as a growth substrate for the microorganisms.

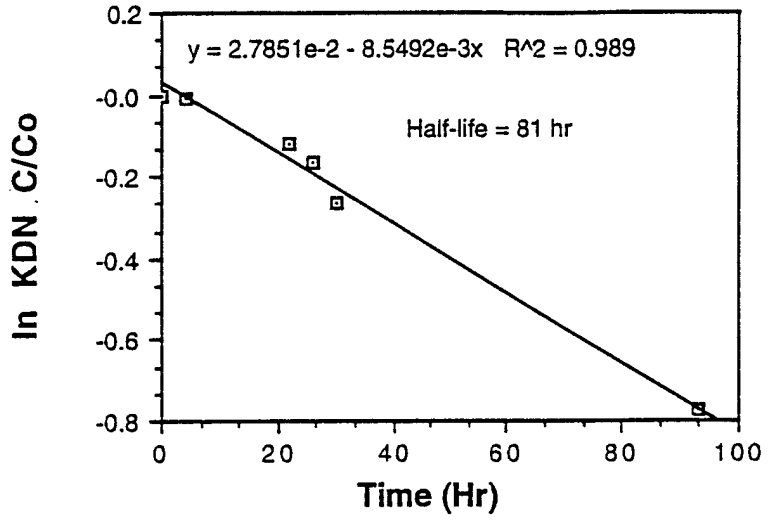

Figure 16. First-order loss plot for KDN.

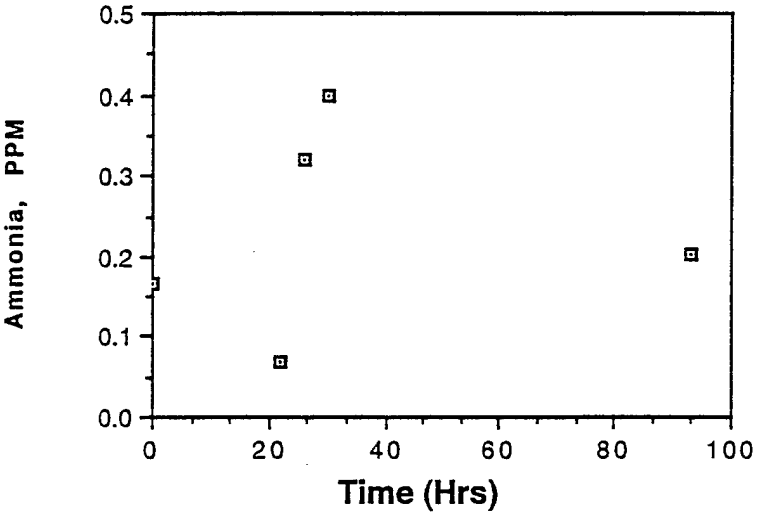

Figure 17. Plot of the formation and decline of ammonia from KDN.

ENVIRONMENTAL FATE OF POLYALKYLPERFLUOROETHERS

Photoreactions of PAPFE

UV absorption by PAPFE should be essentially undetectable in the solar region, based on their structures (see Background). The UV spectrum of neat Fomblin Z (~ 4.8 M) gives absorption cross sections (ε) at 300 nm and 330 nm of 0.01 M^{-1} cm^{-1} and 7 x 10^{-3} M^{-1} cm^{-1} respectively, very nearly at the baseline values. These very low absorption values in the solar region probably are due to carbonyl impurities on end groups. Photoreactions in the solar region,

therefore, should be undetectable over a time period of several months to years. To confirm this conclusion, a quartz tube filled with neat Fomblin Z was exposed to Menlo Park, CA sunlight (lat 38° 40') for seven months without finding any detectable change in the UV spectrum.

Photoreduction Experiments with Fomblin Z

To evaluate the possibility that photoreduction of CF binds in Fomblin Z could be effected using a semiconductor, Fomblin Z was suspended along with 0.1% TiO_2 and 1 mM isopropyl alcohol in water, irradiated with a xenon lamp for several hours and then tested for fluoride ion formation. Photoreduction, using TiO_2 reverses its usual application as photooxidation catalyst by utilizing excited state hole-electron couples to effect reductive cleavage of a -CF bond, simultaneously with oxidation of a sacrificial reductant such as isopropyl alcohol. The relevant reactions are shown below

$$TiO_2 \xrightarrow{h\nu} {}^{\cdot}TiO_2^{+} \qquad (3)$$

$$>CF_2OCF_2\text{-} + {}^{\cdot}TiO_2^{+} + >CHOH \longrightarrow >CF_2OCF\bullet + F^{-} + Ti(OH)O_2 + >\dot{C}HOH \qquad (4)$$

$$>CF_2OCF\bullet + CHOH \longrightarrow >CF_2OCFH + >\dot{C}HOH \qquad (5)$$

$$>CF_2OCF\bullet + O_2 \longrightarrow >CF_2OCFO_2\bullet \longrightarrow \longrightarrow >CF_2OC(=O)F \qquad (4)$$

$$>CF_2OCF\bullet \longrightarrow >CF_2\bullet + O{=}CF\text{-} \qquad (6)$$

A series of experiments used 0.25 mmoles Fomblin Z in 100 mL MilliQ water with 1.1 mmoles i-PrOH in argon or air and photolyzed for 4 hrs using a xenon (solar) lamp. The reaction mixtures were analyzed at several times for fluoride ion by ion chromatography, but no fluoride ion was detected in any mixture above the background value. Standard injections of fluoride ion indicated a detectability limit for fluoride ion of almost 5 μM. If only one PAPFE CF group were reduced to fluoride ion in these mixtures, the concentration of fluoride ion would be 2500 μM. On that basis, TiO_2 photoreduction produced less than 0.2% reaction.

The chief experimental difficulty in reducing PAPFE with TiO_2 is ensuring that the ether has sufficient contact with TiO_2 particles to allow interaction of PAPFE with surface electrons. The same issue of contacting the Fomblin Z with enzyme centers arises in biodegradation (see below).

Biotransformations

This investigation was conducted to determine the potential for Fomblin-Z (III) to undergo biotransformation in aerated or anaerobic sediments. Since analysis for loss of III in water is not possible, fluoride ion, generated by enzymatic hydrolysis of the perfluoroether unit or enzymatic replacement of organic fluoride by hydride ion was monitored by ion chromatographic methods. Sediments samples from a nearby pond were collected and admixed with Fomblin Z (40 mg/75 g sediment) and basal salts medium. Sediments were flushed either with nitrogen or air for up to 220 days, during which time samples were periodically removed and analyzed for fluoride ion. The analytical results for the anaerobic samples are shown in Table 8.

Table 8

FLUORIDE ION PRODUCTION DURING ANAEROBIC BIOTRANSFORMATION OF FOMBLIN-Z

Time, days	Fluoride, ppm
0	0.0
7	0.0
14	0.0
31	0.0
71	1.2
111	1.4
220	2.2

During the course of the study, the soil remained dark, which is typical of soil in anaerobic environments. A lag phase of 71 days was observed before the appearance of fluoride ion. Increases in fluoride concentration were observed up to day 220 when the study was terminated. A plot of the Table 8 data appears in Figure 18. The data suggest an initial increase in fluoride ion between Days 31 and 71 followed by more linear fluoride ion production. If Fomblin-Z is

approximately 58% fluorine, then total mineralization would yield 116 ppm fluoride ion in solution. In the study time period, only 1.9% conversion was observed.

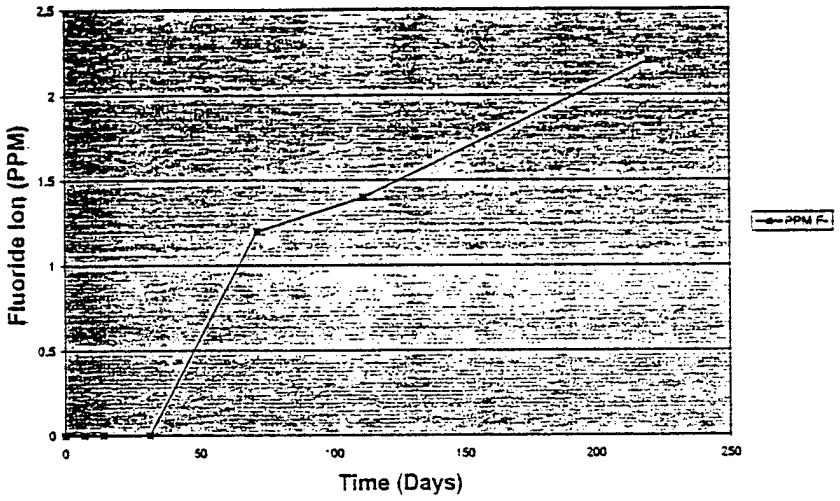

Figure 18. Formation of fluoride ion as a function of time under anaerobic condtions.

A zero-order kinetic analysis was applied to the data after the 71-day lag phase. A zero-order rate constant of 5.9×10^{-3} % Day^{-1} was determined. From this rate constant, half of the original Fomblin Z in anaerobic sediment would be transformed in 8500 days or 23 years. A similar evaluation was conducted for aerobic biotransformation, with the results shown in Table 9.

Table 9

FLUORIDE ION PRODUCTION DURING AEROBIC BIOTRANSFORMATION OF FOMBLIN-Z

Time, days	Fluoride, ppm
0	0.0
7	0.0
14	0.0
31	0.0
64	0.0
104	0.37
206	0.67

In this case, the lag phase was longer and fluoride ion began to appear only after 104 days. The sediment in this study appeared much lighter in color than those observed in the anaerobic study. A doubling of fluoride ion concentration at 206 days suggests a zero-order formation process as was observed in the anaerobic case. However, due to time constraints, sufficient data could not be collected for a reliable kinetic analysis.

An estimate of the aerobic biotransformation rate of Fomblin-Z of approximately one-third that of the anaerobic process is reasonable. The slow transformation rates probably were the result of the extremely low solubility of Fomblin Z in water, preventing effective contact with the microorganisms. Microorganisms can generate surfactants to help solubilize such highly insoluble materials, but with PAPFEs, this strategy may have been of little value because of the low percentage of carbon (18%) available in Fomblin-Z for microbial growth. The observed difference in rates between the anaerobic and aerobic Fomblin-Z test systems further strengthened the belief that the observed transformation was biotic and typical of halogenated aliphatic chemicals in sediment.

DISCUSSION

PHOTOLYSIS RATES AND PATHWAYS

The aqueous photoprocess can be described as a combination of two or more reactions, possibly involving water in at least one pathway. Reaction (8), intramolecular O-atom transfer in the ADN excited state from one nitro group to the other to form N2O and NO_3^- is the simplest explanation for formation of these two products in water. Reaction (9) simply accounts for the increasing proportion of NO_2^- ion formed with increasing pH, but does not indicate the detailed pathway.

$$^-N(NO_2)2 + h\nu \longrightarrow {}^-N(NO_2)2^* \quad (7)$$

$$^-N(NO_2)2^* \longrightarrow NO_3^- + N_2O \quad (8)$$

$$HO^- + 2N(NO_2)_2^- + h\upsilon \longrightarrow 4NO_2^- + N_2O + H^+ \quad (9)$$

To determine whether O-atom transfer was intra- or intermolecular, the concentration of ADN in aerated, pH 3 water was varied over a 50 fold range with the ratios of N_2O to NO_3^- and NO_2^- to NO_3^- unchanged and close to 1 and 0.45 respectively, confirming that the intramolecular O-atom transfer pathway is the major process for forming N_2O and NO_3^- in water. The effect of increasing pH increasing the NO_2^-/NO_3^- ratio is more difficult to account for. One possibility involves protonation of excited state DN^- to give $O_2NN{=}NO_2H$ which has a much higher pK_a than the corrresponding ground state acid. Subsequent reactions of this acid with HO^- can be postulated to give NO_2^-

$$^-N(NO_2)_2^* + H^+ \longrightarrow O_2NN{=}NO_2H^* \quad (10)$$

$$O_2NN{=}NO_2H^* + HO\text{-} \longrightarrow O_2NN(OH)\text{-}NO_2H^- \quad (11)$$

$$O_2NN(OH)\text{-}NO_2H^- + H_2O \longrightarrow \longrightarrow 3NO_2^- + 3H^+ \quad (12)$$

This sequence accounts for the higher proportion of NO_2^- and lesser proportion of N_2O and NO_3^- formed at high pH (Tables 4 and A-1), but Reactions (10) -(12) have no supporting evidence. An alternative sequence might involve initial homolysis of the N-N bond of $^-N(NO_2)_2^*$, followed by rapid hydrolysis of NO_2 to form NO_3^- and NO_2^- ,with more NO_3^- at low pH, and more NO_2^- at high pH.

$$^-N(NO_2)_2^* \longrightarrow {}^-O_2NN + NO_2 \qquad (13)$$

$$2NO_2 + H_2O \longrightarrow NO_3^- + NO_2^- + 2H^+ \qquad (14)$$

However, experiments (not shown) on hydrolysis of NO_2 in water indicate that the ratio of NO_2^-/NO_3^- is close to 1, over the entire pH range of 2-11, seemingly ruling out NO_2 as a major source of NO_3^- or NO_2^-. Figure 19 depicts some possible hydrolytic routes to products by interactions of water and HO^- with excited DN^- anion.

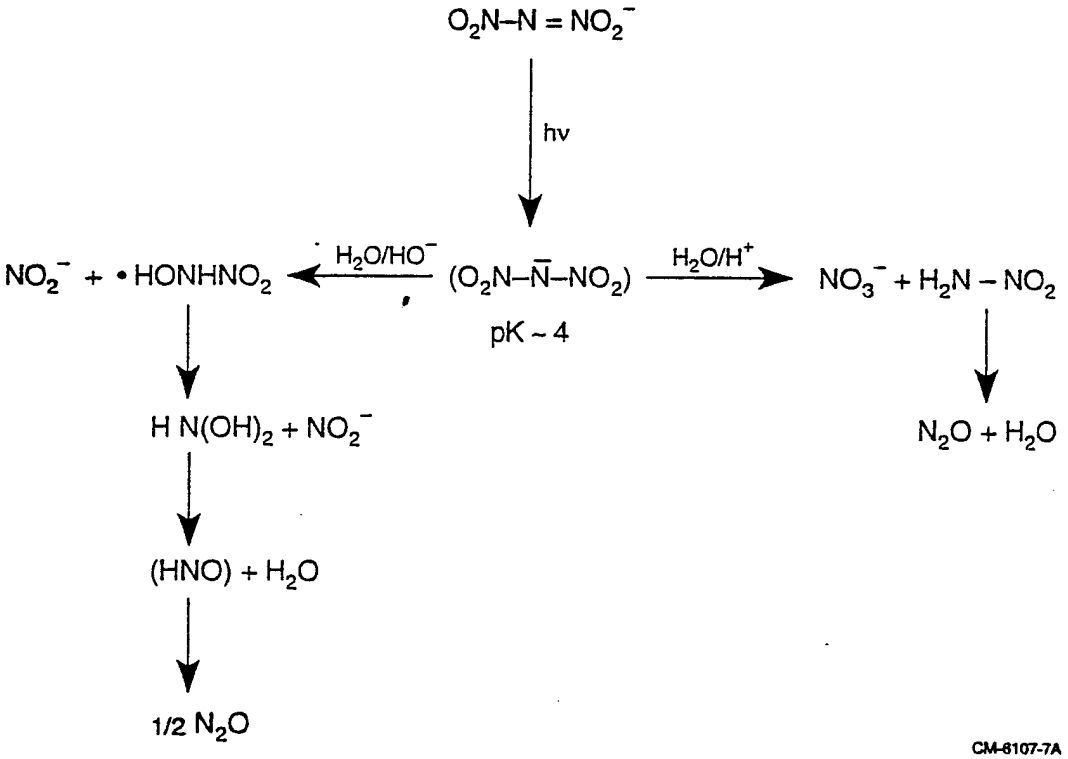

Figure 19. Aqueous DN^- photolysis pathways.

The rapid and similar photolysis rates for photolysis of ADN in organic solvents and in water indicates that the quantum yields for photolysis are high in all of the solvents and that in acetone triplet sensitization also is important. This observation could mean that although indirect photolysis by excited humic species cannot compete with the direct process in natural waters (Beretvas et al., 1995), triplet sensitization in soils or sediments could become important when humic or sediments compete more effectively with ADN for photons.

Solid state photoreactions of ADN and KDN differ from those in aqueous solution in two important ways: significant amounts of NO form in the solid films, but not in water and solid ADN (but not KDN) solid gives little or no NO_2^-, but does form N_2 and water with concomitant loss of NH_4^+ and NO_2^-. No NO_2 was detected by IR spectroscopy indicating that less than 1% of photolyzing ADN gives NO_2. Photolysis of ^{15}N -center labeled ADN gave enough ^{15}NNO to account for half the initial ^{15}N . The remaining ^{15}N apparently was located in $^{15}N^{14}N$ formed from NH_4^+ and $15NO_2^-$.

The same intramolecular O-atom transfer shown in Reaction (8) to give equimolar amounts of N_2O and NO_3^- also appears to be important in the solid state. Tables A.2 and A.3 show that nearly equal amounts of these products form from both ADN and KDN.

\Homolysis or heterolysis of the N-N bond is a likely primary photochemical event in solution or in the solid state, probably originating with the triplet DN-, either with or followed by rapid electron transfer to give NNO_2 and NO_2^-. Formation of free NO_2 is ruled out by its absence in the solid ADN photolysis product mixture and rearrangement of NNO_2 to give two NO is ruled out by the absence of any ^{15}N in NO formed. Another pathway involving initial N-N cleavage, followed by reformation of a N-O bonded ADN isomer (O_2N-N-ONO) could also lead to NO_2^- and two NO, but efforts to isolate the nitrite ester at low temperature were unsuccessful. Figure 20 depicts the reaction scheme which only partly accounts for the experimental data.

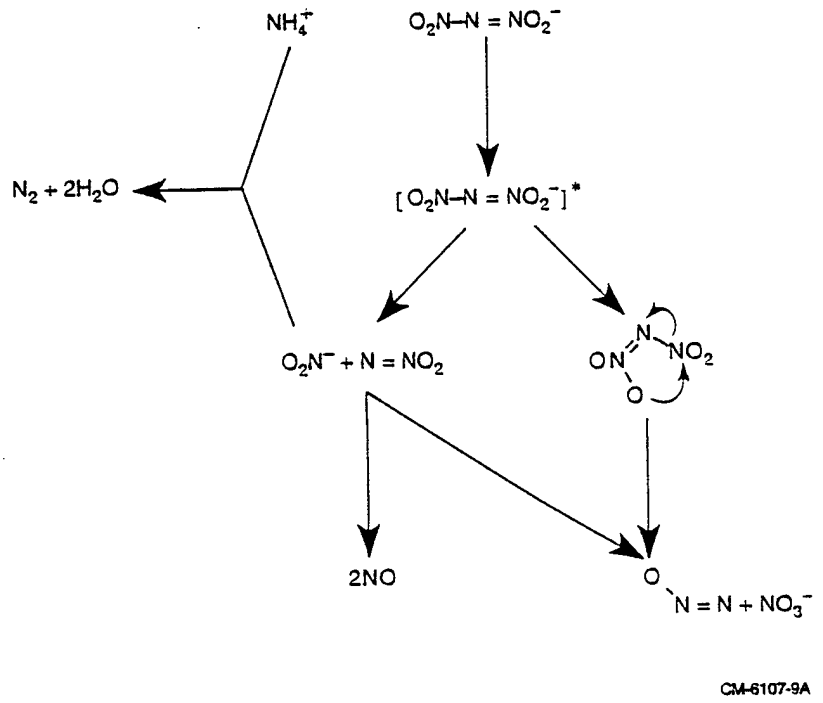

Figure 20. Pathway for solid ADN photolysis

EXPERIMENTAL

MATERIALS

ADN, KDN, and $Li^{15}NO_3$ were supplied by J. Bottaro of SRI as 98+% pure materials. Fomblin Z and Demnum PAPFEs were supplied by L. Gschwender of Wright Patterson AFB. Organic solvents were used as supplied by Aldrich Chemical Co. Purified argon, NO and NO_2 were supplied by SCOTT GASES. ^{15}N-ADN wAS provided by L. Merwin of China Lake NWC, Ridgecrest, CA. Samples of $^{15}NO_2$, ^{15}NNO, and $N^{15}NO$ were prepared as needed by pyrolyzing $Li^{15}NO_3$, $^{15}NH_4NO_3$ or $NH_4{}^{15}NO_3$ in an FTIR cell using a heat gun. The $Li^{15}NO_3$ was provided by J. Bottaro of SRI; $^{15}NH_4NO_3$ and $NH_4{}^{15}NO_3$ were purchased from Cambridge Isotopes, Inc.

ANALYTICAL METHODS

ADN Measurements

High performance liquid chromatography (HPLC) was used to measure ADN and KDN cocnentrations in solutions. Conditions for HPLC analyses included use of a Hewlett Packard Series 1090 LC equipped with UV detector, autosampler, and HP Chemstation software. The operating conditions for the systems were:

Column:	HP, ODS, 5 μ, 250 x 4.6 mm and equivalent guard column; 40°C.
Mobile Phase:	40% acetonitrile/60% TBAH (Tetrabutylammonium hydroxide, 50 mM)
Flow Rate:	1.0 mL/min
Detection:	290 nm
Injection:	100 μL
Run Time:	10 min
Retention Time:	4.2 min

Nitrate and Nitrite Measurements

Ion chromatography (IC) was used for NO_3^- and NO_2^- analyses. The system included a Dionex 2000I IC equipped with Conductivity detector, autosampler, and Peaknet software. The operating conditions for the system:

Column:	Dionex OmniPac PAX-500 with guard column.
Mobile Phase:	50mM NaOH
Flow Rate:	1.0mL/min
Detection:	Conductivity with anion suppressor, 25 mN H_2SO_4, 5mLmin
Injection:	50 µL Loop
Run Time:	10 min
Retention times:	3.27 min NO_2^-; 4.90 min NO_3^-

Fluoride Ion

Fluoride ion was analyzed by capillary ion analysis using a Waters Quanta 4000 Capillary Ion Analyzer under the following conditions:

Electrolyte:	4.6 mM sodium chromate, 0.46 osmotic flow modifier (a Waters supplied material added to the electrolyte).
Column:	60 cm x 75 m fused silica capillary
Applied voltage:	20 kv after isomigration conditioning.
Current range:	18-20 A. Injection mode: Hydrostatic at 10 cm for 30 sec
Detection:	HYPERLINK mail to: Uv@254 (indirect photometric)
Retention time:	Fluoride ion: 9.7 min; chloride ion: 7.7 min

A capillary ion chromatogram for the starting soil extract appears in Figure 21 and the extract spiked with 1 ppm fluoride ion appears in Figure 22.

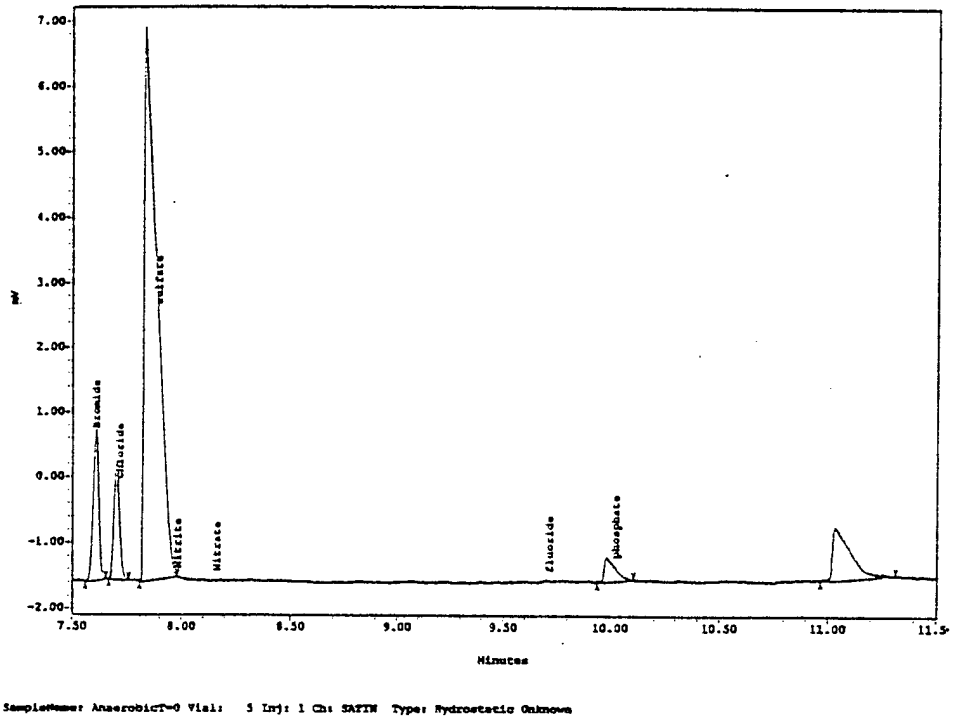

Figure 21. Starting soil extract ion chromatogram.

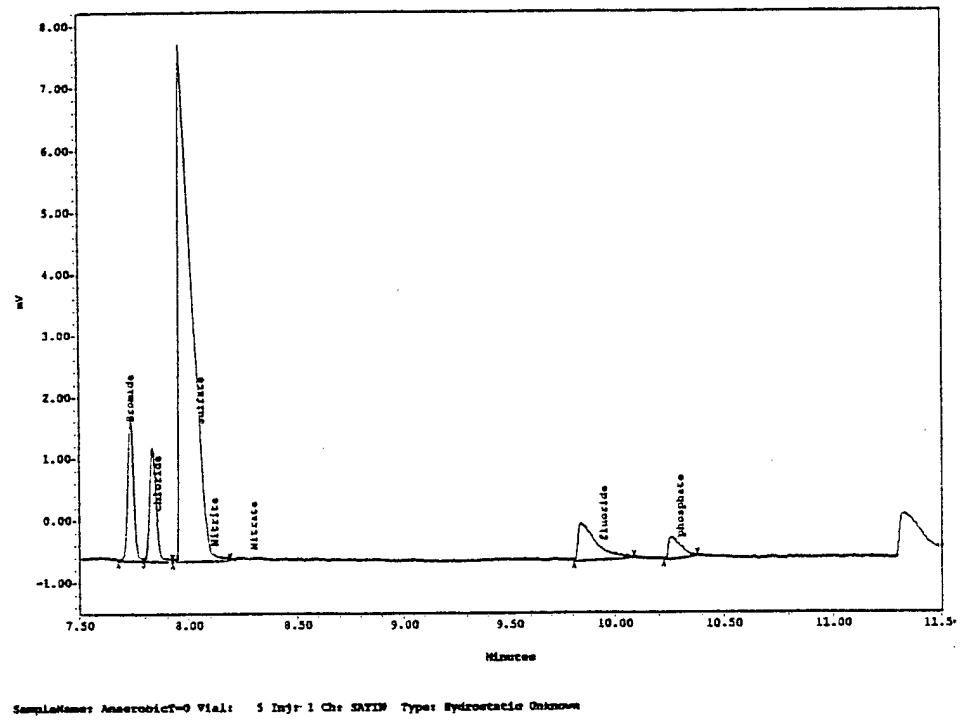

Figure 22. Soil extract spiked with 1 ppm fluoride ion.

Gas Analyses

Gas chromatography was used to analyze for N_2O, NO and N_2. The system included a Hewlett Packard Series 6890 GC equipped with TCD detector and HP Chemstation software.

Operating Conditions:

Column:	Alltech, Porapak Q 80/100, 12'x1/8" and MP-1, 100120, 30'x1/8" connected with a column switch valve
Column switch:	GC Start as Porapak Q then MP-1, and turn switch on at 4 minute then the column order are reversed
Carrier gas:	Helium
Oven Temp.:	50°C
Flow Rate:	18mL/min
Detection:	Conductivity, 250°C
Injection:	200 µL
Run Time:	25 min
Retention times:	CO_2, 6.199 min; N_2O, 8.16 min; N_2, 12.85 min; NO, 14.42 min

ACTINOMETRY

Quantum yields for aqueous ADN photolysis reactions were determined using potassium ferrioxalate (KFO) solutions and following procedures described by Calvert and Pitts (1968). Solid ADN actinometry used a special borosilicate window coated with a thin film of ADN cast from methanol in front of a square 1 cm UV cell containing KFO solution. Figure 23 shows the arrangement of the window and cell.

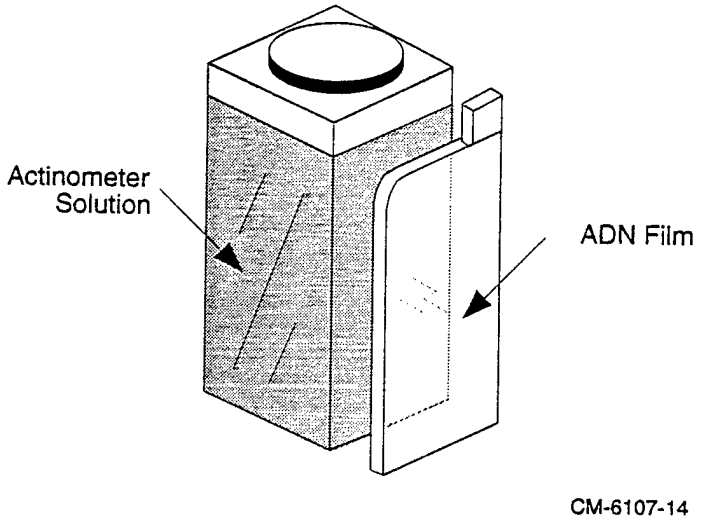

Figure 23. Optical cell arrangement for ADN solid film actinometry.

FTIR GAS MEASUREMENTS

A 500 mL IR cell (8 cm dia) with detachable NaCl windows and twin stopcocks was used as the photolysis cell by inserting a 5 cm dia borosilicate cylinder coated with a 1 μm ADN or KDN film, flushing the cell with argon or CO_2 and photolyzing the film using a 450 W xenon lamp. Following photolysis, the IR spectrum was measured using a FT 20 FTIR spectrometer. Figure 24 illustrates the arrangement of the ADN film in the IR cell.

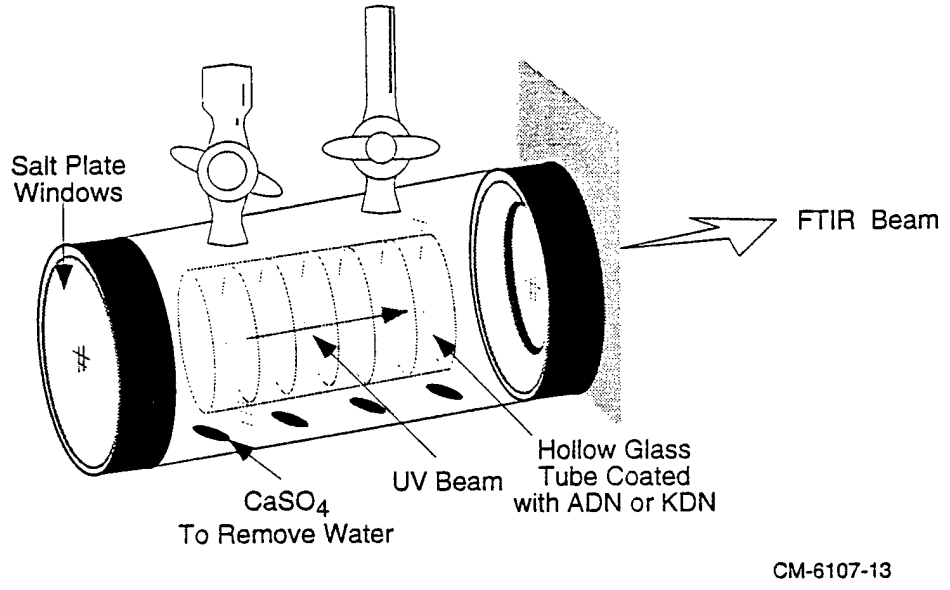

Figure 24. IR cell with internal thin film for FTIR analysis of gaseous products.

PHOTOLYSIS SYSTEMS

Sunlight and xenon lamp photolysis experiments conducted in 10 mL quartz tubes sealed with caps fitted with stopcocks and Teflon-lined septa for aqueous samples and 100 mL borosilicate cylindrical vessels for solid thin films. Gas samples were withdrawn from the head space with corrections for gas solubilities made using Henry's constants for N_2O and NO in water.

Narrow wavelength photolyses were conducted with an optical bench and an Oriel 1/4 m monochrometer and 450 W xenon lamp.

FOMBLIN BIODEGRADATION TESTS

Tests were performed in 200 mL Schott jars with screw-capped sealed tops equipped with gas inlet and outlet lines. The inlet line was connected to a nitrogen gas cylinder for the anaerobic study and the outlet line was connected to a glycerol U-tube and the nitrogen flow was adjusted to maintain a positive pressure. For the aerobic study, the inlet line was connected to the house air system, filtered through glass wool prior to entering the flask, and a glycerol U-tube was used to maintain a positive pressure and to check gas flow.

Pond sediment from Searsville Pond, a local eutrophic water body located at Jasper Ridge Ecological Preserve near Stanford University,was used as the source of microbial populations. Seventy five g of wet sediment.was added to each test jar along with 40 mg of Fomblin-Z. The mixture was stirred with a metal spatula as 180 mL of basal salts medium was added, then the jar was capped and gas flow started. The jar was shaken periodically by hand. Aqueous samples were collected periodically by removal of the gas exit line and using a syringe to extract a 1.5 mL sample under positive gas flow. The water sample was filtered through a 0.45 μm filter prior to analysis by capillary electrophoresis.

Fomblin-Z was added directly to the sediment because no suitable solvent was found to effectively solubilize the PAPFE. Solvents tested included water, dimethylformamide, dimethylsulfoxide, acetone, dichloromethane, diethyl ether, dioxane, tetrahydrofuran, glacial acetic acid, and ethyl acetate.

REFERENCES

AFOSR. 1994. Fate Assessment of New Air Force Chemicals. Air Force Office of Scientific Research. Contract 49620-94-C-0031,

Beretvas, M., S. Burns, J. P. Hassett. 1995. Effects of Humics on the Photodegradation of ADN. Div. Environ. Chem. Preprint papers, 210th ACS Natl. Meet., Chicago, IL, August 20-24, pp. 598-600.

Borman, S. 1994. Advanced energetic materials emerge from military and space applications. Chem. Eng. News 17 Jan., pp 18-22.

Calvert, J. and J. Pitts. 1968. Photochemistry, John Wiley and Sons, New York, N.Y.

Mill, T., M. Su, D. Yao and R. Spanggord. 1995. Fate Assessment of New Air Force Chemicals. Annual Report. AFOSR Contract No. F49620-94-C-0031.

Schmitt, R., J. C. Bottaro, D. S. Ross and P. E. Penwell. 1991,1993. Dinitramide Salts and Method of Making Same, U.S. Patent No. 5,254,324, issued October 19, 1993. International patent application No. WO 91/19669, published Dec. 26, 1991

Yao, C.C. D., M. Su and T. Mill. 1995. Photolysis Rates and Pathways for Dinitramide Ion, Div. Environ. Chem. Preprint papers, 210th ACS Natl. Meet., Chicago, IL, August 20-24, pp. 514-518

Zepp, R. G., and D. M. Cline. 1977. Rates of direct photolysis in aquatic environments. Environ. Sci. Technol. 11: 359-365.

APPENDIX

TABLE A1

EFFECT OF pH ON RATES AND PRODUCTS OF THE PHOTOLYSIS OF AQUEOUS ADN IN AIR[a]

pH Value	ADN Init. µmoles	Δ ADN µmoles	10^3 k_p, sec^{-1}	N_2O[b] µmoles	NO_2^- µmoles	NO_3^- µmoles	NO_2^-/NO_3^- Ratio	Sum N[c] µmoles	N Mass[d] Balance, %
pH 2	2.30	1.91	7.3	1.78	0.567	2.05	0.28	6.18	108
pH 3	2.19	1.82	7.2	1.67	0.928	2.01	0.46	6.28	115
pH 5	2.3	1.60	4.9	1.12	2.07	0.943	2.2	5.25	109
pH 7	2.31	1.51	4.4	0.965	2.36	0.539	4.4	4.83	106
pH 9	2.22	1.40	4.2	0.762	2.61	0.385	6.8	4.52	107
pH 11	2.19	1.34	3.9	0.784	2.68	0.199	13	4.45	111
pH 12	2.22	1.31	3.3	0.534	2.87	0.171	41	4.11	104

[a]Solutions were 0.115-0.109 mM in ADN; 20 mL of ADN solution photolyzed with LX300 xenon lamp for 4 min in quartz tubes with 14 mL headspace.

[b]Calculated from Henry's law: [C]g, ppmv/[C], µM = 32.5.

[c]Calculated from $2N_2O + NO_2^- + NO_3^-$.

[d]Calculated from Sum N/ΔADN.

Table A2

EFFECT OF pH ON RATES AND PRODUCTS OF THE PHOTOLYSIS OF AQUEOUS KDN IN AIR AND ARGON
(All concentration units in μmoles)

pH Value	KDN Init.	Δ KDN	10^3 kp, s^{-1}[b]	N_2O[b]	NO_2^-	NO_3^-	NO_2^-/NO_3^-	NO_2^-/NO_3^- Ratio	Σ N[c]	N Mass[d] Balance, %
AIR										
pH 2	2.264	1.87	7.3	1.618	0.596	2.02	2.619	0.295	5.86	104
pH 3	2.223	1.79	6.8	1.600	0.837	1.97	2.812	0.424	6.01	111
pH 11	2.284	1.27	3.4	0.545	2.3	0.182	2.484	12.68	3.57	93
pH 12	2.251	1.21	3.2	0.457	2.38	0.144	2.520	16.56	3.44	94
ARGON										
pH 2	2.246	1.814	6.8	1.633	1.409	1.16	2.565	1.22	5.83	107
pH 3	2.313	1.862	6.8	1.490	1.361	1.45	2.808	0.94	5.79	103
pH 11	2.292	1.377	3.8	0.748	2.653	0.379	3.031	7.01	4.53	110
pH 12	2.294	1.316	3.6	0.518	2.805	0.351	3.156	7.99	4.19	106

[a]Solutions were 0.115-0.109 mM in KDN; 20 mL of KDN solution photolyzed with LX300 xenon lamp for 4 min in quartz tubes with 14 mL headspace.
[b]Calculated from Henry's law: [C]g, ppmv/[C], μM = 32.5.
[c]Calculated from $2N_2O + NO_2^- + NO_3^-$.
[d]Calculated from Sum N/ΔKDN.

Table A3

PHOTOLYSIS OF ADN THIN FILMS IN CO_2[a]
(All concentration units in μmoles)

ADN init.	ADN Final	Δ ADN	N_2O	N_2	NO	NO_2^-	NO_3^-	NH_4^+ consum	ΣN	N mass Bal %
19.35	13.69	5.66	1.85	6.97	2.66	2.24	2.46	3.57	17.42	84.8
19.35	6.40	12.95	5.92	11.56	4.64	1.86	8.04	6.18	41.89	93.0
19.35	3.53	15.82	7.54	11.79	8.12	2.17	11.69	6.49	53.04	98.3
19.35[b]	19.32	0.04	0.00	3.80	0.00	0.00	0.00	0.00	0.00	0.0
19.35[b]	19.24	0.11	0.00	3.28	0.00	0.00	0.00	0.00	0.00	0.0

[a]Photolyzed 0.1-0.2 μm films under CO_2 using a 450 W xenon lamp in 34 mL quartz tubes for 40 or 60 min.
[b]Dark control.

Table A4

PHOTOLYSIS OF KDN THIN FILMS IN CO_2[a]
(All concentration units in μmoles)

KDN init.	KDN Final	Δ KDN	N_2O	N_2•	NO	NO_2^-	NO_3^-	ΣN	N mass Bal %
14.07	4.73	9.34	3.29	4.16	4.35	6.56	5.67	23.15	82.7
14.07	4.52	9.55	3.74	4.07	7.73	7.28	5.26	27.75	96.9
14.07	3.72	10.35	3.34	9.98	6.63	7.58	6.90	27.78	89.5
14.07[b]	14.07	0.00	0.00	9.40	0.00	0.00	0.00	0.00	0.0
14.07[b]	14.19	-0.12	0.00	3.42	0.00	0.00	0.00	0.00	0.0

[a]Photolyzed 0.1-0.2 μm films under CO_2 using a 450 W xenon lamp in 34 mL quartz tubes for 40 or 60 min.
[b]Dark control.

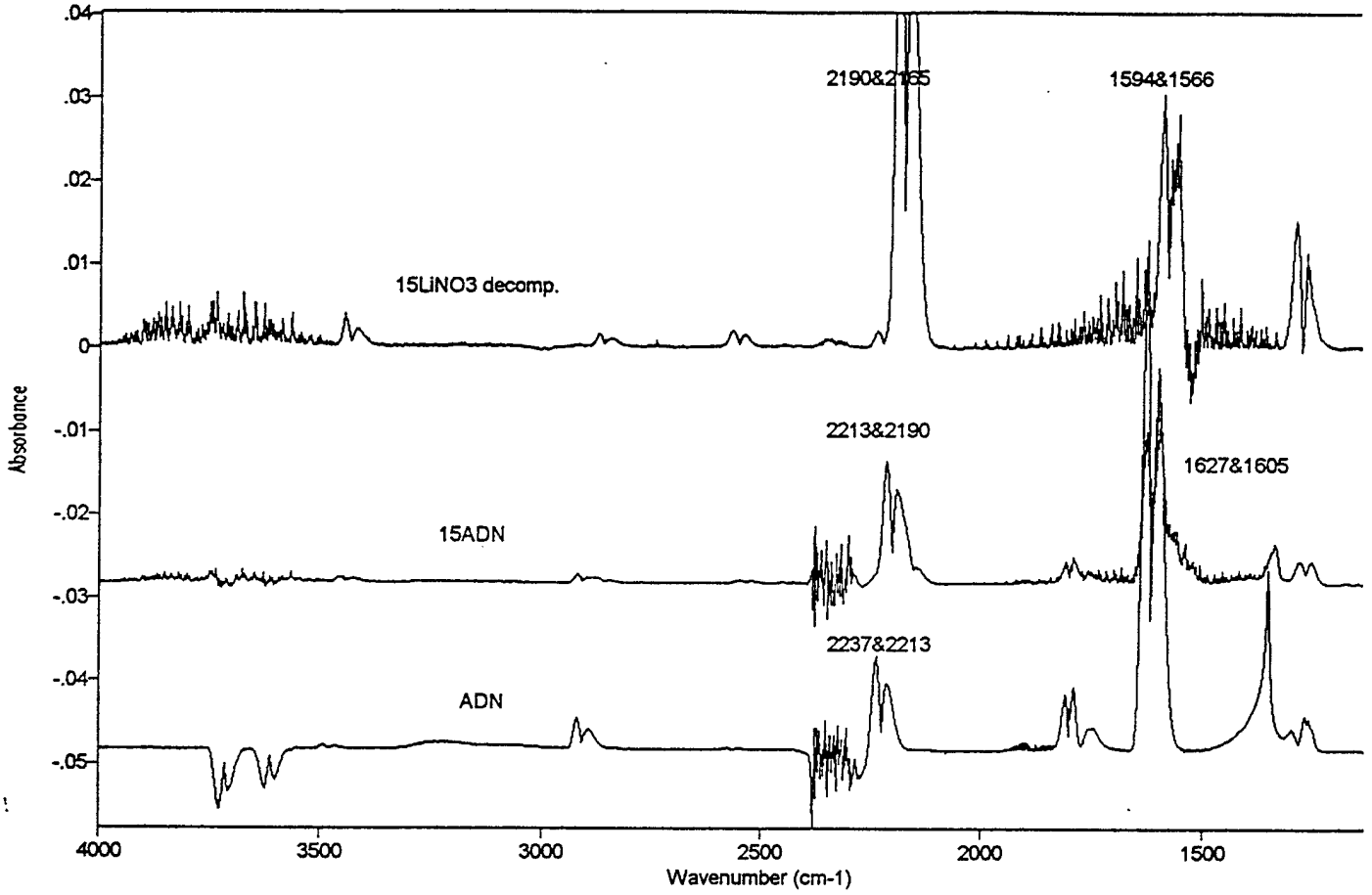

Figure A1. IR spectra of NO_2 derived from ADN ($^{14}NO_2$), ^{15}N-ADN ($^{14}NO_2$) and Li $^{15}NO_3$ ($^{15}NO_2$), all at 1627 to 1566 cm^{-1}. Peaks at 2237 to 2165 cm^{-1} are from N_2O impurities.